ESAIM: M2AN 51 (2017) 509–535
DOI: 10.1051/m2an/2016032

ESAIM: Mathematical Modelling and Numerical Analysis
www.esaim-m2an.org

DIVERGENCE FREE VIRTUAL ELEMENTS FOR THE STOKES PROBLEM ON POLYGONAL MESHES

Lourenco Beirão da Veiga[1], Carlo Lovadina[2,3] and Giuseppe Vacca[4]

Abstract. In the present paper we develop a new family of Virtual Elements for the Stokes problem on polygonal meshes. By a proper choice of the Virtual space of velocities and the associated degrees of freedom, we can guarantee that the final discrete velocity is *pointwise* divergence-free, and not only in a relaxed (projected) sense, as it happens for more standard elements. Moreover, we show that the discrete problem is immediately equivalent to a reduced problem with *fewer* degrees of freedom, thus yielding a very efficient scheme. We provide a rigorous error analysis of the method and several numerical tests, including a comparison with a different Virtual Element choice.

Mathematics Subject Classification. 65N30, 65N12, 65N15, 76D07.

Received October 6, 2015. Revised March 3, 2016. Accepted April 21, 2016.

1. Introduction

The last decade has seen an increased interest in developing numerical methods that can make use of general polygonal and polyhedral meshes, as opposed to more standard triangular/quadrilateral (tetrahedral/hexahedral) grids. Indeed, making use of polygonal meshes brings forth a range of advantages, including for instance automatic hanging node treatment, more efficient approximation of geometric data features, better domain meshing capabilities, more efficient and easier adaptivity, more robustness to mesh deformation, and others. This interest in the literature is also reflected in commercial codes, such as CD-Adapco, that have recently included polytopal meshes.

We refer to the recent papers and monographs [6,10,15,17,20,21,24,31,39,41–47,50,51] as a brief representative sample of the increasing list of technologies that make use of polygonal/polyhedral meshes. We mention here

Keywords and phrases. Virtual element method, polygonal meshes, Stokes problem, divergence free approximation.

[1] Dipartimento di Matematica e Applicazioni, Università degli Studi di Milano Bicocca, Via Roberto Cozzi 55, 20125 Milano, Italy. lourenco.beirao@unimib.it

[2] Dipartimento di Matematica, Università degli Studi di Pavia, Via Ferrata 1, 27100 Pavia, Italy.

[3] IMATI-CNR, Via Ferrata 1, 27100 Pavia, Italy. carlo.lovadina@unipv.it

[4] Dipartimento di Matematica, Università degli Studi di Bari, Via Edoardo Orabona 4, 70125 Bari, Italy.
giuseppe.vacca@uniba.it

Article published by EDP Sciences

in particular the polygonal finite elements, that generalize finite elements to polygons/polyhedrons by making use of generalized non-polynomial shape functions, and the mimetic discretisation schemes, that combine ideas from the finite difference and finite element methods.

The Virtual Element Method (in short, VEM) has been recently introduced in [7] as a generalization of the finite element method to arbitrary element-geometry. The principal idea behind VEM is to use approximated discrete bilinear forms that require only integration of polynomials on the (polytopal) element in order to be computed. The resulting discrete solution is conforming and the accuracy granted by such discrete bilinear forms turns out to be sufficient to achieve the correct order of convergence. Following this approach, VEM is able to make use of very general polygonal/polyhedral meshes without the need to integrate complex non-polynomial functions on the elements and without loss of accuracy. Moreover, VEM is not restricted to low order converge and can be easily applied to three dimensions and use non convex (even non simply connected) elements. The Virtual Element Method has been developed successfully for a large range of problems, see for instance [1–4, 7, 8, 12, 14, 19, 22, 34, 40, 49]. A helpful paper for the implementation of the method is [9].

The focus of this paper is on developing a Virtual Element Method for the Stokes problem. For such a problem, a few other numerical schemes using polytope meshes have been proposed, see for example [5, 27, 38, 52]. In [8] the authors presented a family of Virtual Elements for the linear elasticity problem that are locking-free in the incompressible limit. As a consequence, the scheme in [8] can be immediately extended to the Stokes problem, thus yielding a stable VEM family that would be comparable to the Crouzeix–Raviart finite element family.

In the present paper, we develop a new Virtual Element Method for the Stokes problems by exploiting in a new way the flexibility of the Virtual Element construction. In particular, we define a new Virtual Element space of velocities carefully designed to solve the Stokes problem. In connection with a suitable pressure space, the new Virtual Element space leads to an exactly divergence-free discrete velocity, a favorable property when more complex problems, such as the Navier–Stokes problem, are considered. We highlight that this feature is not shared by the method defined in [8] or by most of the standard mixed Finite Element methods, where the divergence-free constraint is imposed only in a weak (relaxed) sense. We however remark that, using different discretization methodologies, some divergence-free methods have already proposed in the literature (for instance, see [23, 25, 28, 29, 35, 36]).

In addition to the above feature, the proposed method carries an additional important advantage. By selecting suitable degrees of freedom (DoFs in the sequel), we obtain an automatic orthogonality condition among many pressure DoFs and the associated DoFs for the velocities. As a consequence, a large amount of degrees of freedom can be automatically eliminated from the system and one obtains a new reduced problem with less degrees of freedom: only one pressure DoF per element and very few internal-to-elements DoFs for the velocities. We finally note that the proposed problem is new also on triangles and quadrilaterals, allowing for new divergence-free (Virtual) elements with fewer degrees of freedom.

In brief, the proposed family of Virtual Elements has three advantages: (1) it can be applied to general polygonal meshes; (2) it yields an exactly divergence-free velocity; (3) it is efficient in terms of number of degrees of freedom. In the current work, after developing the method, we prove its stability and convergence properties. Finally, we test the method on some benchmark problems and compare it with the Stokes extension of [8].

The paper is organized as follows. In Section 2 we introduce the model continuous Stokes problem. In Section 3 we present its VEM discretisation. In Section 4 we detail the theoretical features and the convergence analysis of the problem. In Section 5 we describe the reduced problem and its properties, while in Section 6 we show the numerical tests. Finally, in the Appendix we briefly describe the extension of the method to the three-dimensional case.

2. The continuous problem

We consider the Stokes problem on a polygon $\Omega \subseteq \mathbb{R}^2$ with homogeneous Dirichlet boundary conditions:

$$\begin{cases} \text{find } (\mathbf{u}, p) \text{ such that} \\ -\nu\,\boldsymbol{\Delta}\mathbf{u} - \nabla p = \mathbf{f} & \text{in } \Omega, \\ \operatorname{div} \mathbf{u} = 0 & \text{in } \Omega, \\ \mathbf{u} = 0 & \text{on } \Gamma = \partial\Omega, \end{cases} \tag{2.1}$$

where $\mathbf{u}$ and p are the velocity and the pressure fields, respectively. Furthermore, $\boldsymbol{\Delta}$, div, $\boldsymbol{\nabla}$, and ∇ denote the vector Laplacian, the divergence, the gradient operator for vector fields and the gradient operator for scalar functions. Finally, $\mathbf{f}$ represents the external force, while ν is the viscosity.

Let us consider the spaces

$$\mathbf{V} := \left[H_0^1(\Omega)\right]^2, \qquad Q := L_0^2(\Omega) = \left\{ q \in L^2(\Omega) \quad \text{s.t.} \quad \int_\Omega q \,\mathrm{d}\Omega = 0 \right\} \tag{2.2}$$

with norms

$$\|\mathbf{v}\|_1 := \|\mathbf{v}\|_{[H^1(\Omega)]^2} \quad , \qquad \|q\|_Q := \|q\|_{L^2(\Omega)}. \tag{2.3}$$

We assume $\mathbf{f} \in [H^{-1}(\Omega)]^2$, and $\nu \in L^\infty(\Omega)$ uniformly positive in Ω. Let the bilinear forms $a(\cdot,\cdot)\colon \mathbf{V} \times \mathbf{V} \to \mathbb{R}$ and $b(\cdot,\cdot)\colon \mathbf{V} \times Q \to \mathbb{R}$ be defined by:

$$a(\mathbf{u}, \mathbf{v}) := \int_\Omega \nu\, \boldsymbol{\nabla}\mathbf{u} : \boldsymbol{\nabla}\mathbf{v} \,\mathrm{d}\Omega, \qquad \text{for all } \mathbf{u}, \mathbf{v} \in \mathbf{V} \tag{2.4}$$

$$b(\mathbf{v}, q) := \int_\Omega \operatorname{div} \mathbf{v}\, q \,\mathrm{d}\Omega \qquad \text{for all } \mathbf{v} \in \mathbf{V},\ q \in Q. \tag{2.5}$$

Then a standard variational formulation of problem (2.1) is:

$$\begin{cases} \text{find } (\mathbf{u}, p) \in \mathbf{V} \times Q, \text{ such that} \\ a(\mathbf{u}, \mathbf{v}) + b(\mathbf{v}, p) = (\mathbf{f}, \mathbf{v}) & \text{for all } \mathbf{v} \in \mathbf{V}, \\ b(\mathbf{u}, q) = 0 & \text{for all } q \in Q, \end{cases} \tag{2.6}$$

where

$$(\mathbf{f}, \mathbf{v}) := \int_\Omega \mathbf{f} \cdot \mathbf{v} \,\mathrm{d}\Omega.$$

It is well-known that (see for instance [16]):

- $a(\cdot,\cdot)$ and $b(\cdot,\cdot)$ are continuous, *i.e.*

$$|a(\mathbf{u}, \mathbf{v})| \le \|a\| \|\mathbf{u}\|_1 \|\mathbf{v}\|_1 \qquad \text{for all } \mathbf{u}, \mathbf{v} \in \mathbf{V},$$

$$|b(\mathbf{v}, q)| \le \|b\| \|\mathbf{v}\|_1 \|q\|_Q \qquad \text{for all } \mathbf{v} \in \mathbf{V} \text{ and } q \in Q;$$

- $a(\cdot,\cdot)$ is coercive, *i.e.* there exists a positive constant α such that

$$a(\mathbf{v}, \mathbf{v}) \ge \alpha \|\mathbf{v}\|_1^2 \qquad \text{for all } \mathbf{v} \in \mathbf{V};$$

- the bilinear form $b(\cdot,\cdot)$ satisfies the inf-sup condition, *i.e.*

$$\exists\, \beta > 0 \quad \text{such that} \quad \sup_{\mathbf{v} \in \mathbf{V}\, \mathbf{v} \ne \mathbf{0}} \frac{b(\mathbf{u}, q)}{\|\mathbf{v}\|_1} \ge \beta \|q\|_Q \qquad \text{for all } q \in Q. \tag{2.7}$$

Therefore, problem (2.6) has a unique solution $(\mathbf{u}, p) \in \mathbf{V} \times Q$ such that

$$\|\mathbf{u}\|_1 + \|p\|_Q \le C\, \|\mathbf{f}\|_{H^{-1}(\Omega)}$$

with the constant C depending only on Ω and ν.

3. Virtual formulation for the Stokes problem

3.1. Decomposition and virtual element spaces

We outline the Virtual Element discretization of problem (2.6). Here and in the rest of the paper the symbol C will indicate a generic positive constant independent of the mesh size that may change at each occurrence. Moreover, given any subset ω in $\mathbb{R}^2$ and $k \in \mathbb{N}$, we will denote by $\mathbb{P}_k(\omega)$ the polynomials of total degree at most k defined on ω, with the extended notation $\mathbb{P}_{-1}(\omega) = \emptyset$. Let $\{\mathcal{T}_h\}_h$ be a sequence of decompositions of Ω into general polygonal elements K with

$$h_K := \operatorname{diameter}(K), \quad h := \sup_{K \in \mathcal{T}_h} h_K.$$

We suppose that for all h, each element K in $\mathcal{T}_h$ fulfils the following assumptions:

- (**A1**) K is star-shaped with respect to a ball of radius $\geq \gamma\, h_K$,
- (**A2**) the distance between any two vertexes of K is $\geq c\, h_K$,

where γ and c are positive constants. We remark that the hypotheses above, though not too restrictive in many practical cases, can be further relaxed, as noted in [7].

We also assume that the scalar field ν is piecewise constant with respect to the decomposition $\mathcal{T}_h$, *i.e.* ν is constant on each polygon $K \in \mathcal{T}_h$.

The bilinear forms $a(\cdot,\cdot)$ and $b(\cdot,\cdot)$, the norms $||\cdot||_1$ and $||\cdot||_Q$, can be decomposed into local contributions. Indeed, using obvious notations, we have

$$a(\mathbf{u},\mathbf{v}) =: \sum_{K \in \mathcal{T}_h} a^K(\mathbf{u},\mathbf{v}) \qquad \text{for all } \mathbf{u},\mathbf{v} \in \mathbf{V} \tag{3.1}$$

$$b(\mathbf{v},q) =: \sum_{K \in \mathcal{T}_h} b^K(\mathbf{v},q) \qquad \text{for all } \mathbf{v} \in \mathbf{V} \text{ and } q \in Q, \tag{3.2}$$

and

$$\|\mathbf{v}\|_1 =: \left(\sum_{K \in \mathcal{T}_h} \|\mathbf{v}\|^2_{1,K}\right)^{1/2} \quad \text{for all } \mathbf{v} \in \mathbf{V}, \qquad \|q\|_Q =: \left(\sum_{K \in \mathcal{T}_h} \|q\|^2_{Q,K}\right)^{1/2} \quad \text{for all } q \in Q. \tag{3.3}$$

For $k \in \mathbb{N}$, let us define the spaces

- $\mathbb{P}_k(K)$ the set of polynomials on K of degree $\leq k$,
- $\mathbb{B}_k(K) := \{v \in C^0(\partial K) \quad \text{s.t} \quad v_{|e} \in \mathbb{P}_k(e) \quad \forall \text{ edge } e \subset \partial K\}$,
- $\mathcal{G}_k(K) := \nabla(\mathbb{P}_{k+1}(K)) \subseteq [\mathbb{P}_k(K)]^2$,
- $\mathcal{G}_k(K)^\perp \subseteq [\mathbb{P}_k(K)]^2$ the L^2-orthogonal complement to $\mathcal{G}_k(K)$.

On each element $K \in \mathcal{T}_h$ we define, for $k \geq 2$, the following finite dimensional local virtual spaces

$$\mathbf{V}_h^K := \left\{ \mathbf{v} \in [H^1(K)]^2 \quad \text{s.t} \quad \mathbf{v}_{|\partial K} \in [\mathbb{B}_k(\partial K)]^2\,, \begin{cases} -\nu\, \boldsymbol{\Delta} \mathbf{v} - \nabla s \in \mathcal{G}_{k-2}(K)^\perp, \\ \operatorname{div} \mathbf{v} \in \mathbb{P}_{k-1}(K), \end{cases} \text{for some } s \in L^2(K) \right\} \tag{3.4}$$

and

$$Q_h^K := \mathbb{P}_{k-1}(K). \tag{3.5}$$

We note that all the operators and equations above are to be interpreted in the distributional sense. In particular, the definition of $\mathbf{V}_h^K$ above is associated to a Stokes-like variational problem on K.

It is easy to observe that $[\mathbb{P}_k(K)]^2 \subseteq \mathbf{V}_h^K$, and it holds

$$\dim\left([\mathbb{B}_k(\partial K)]^2\right) = 2 n_K k, \quad \dim\left(\mathcal{G}_{k-2}(K)^\perp\right) = \frac{(k-1)(k-2)}{2}, \tag{3.6}$$

where n_K is the number of edges of the polygon K.

It is well-known (see for instance [33]) that given

- a polynomial function $\mathbf{g}_b \in [\mathbb{B}_k(\partial K)]^2$,
- a polynomial function $\mathbf{h} \in \mathcal{G}_{k-2}(K)^\perp$,
- a polynomial function $g \in \mathbb{P}_{k-1}(K)$ satisfying the compatibility condition

$$\int_K g \,\mathrm{d}\Omega = \int_{\partial K} \mathbf{g}_b \cdot \mathbf{n} \,\mathrm{d}s, \tag{3.7}$$

there exists a unique pair $(\mathbf{v}, s) \in \mathbf{V}_h^K \times L^2(K)/\mathbb{R}$ such that

$$\mathbf{v}_{|\partial K} = \mathbf{g}_b, \quad \operatorname{div} \mathbf{v} = g, \quad -\nu\, \boldsymbol{\Delta} \mathbf{v} - \nabla s = \mathbf{h}. \tag{3.8}$$

Moreover, let us assume that there exist two different data sets

$$(\mathbf{g}_b,\, \mathbf{h},\, g) \quad \text{and} \quad (\mathbf{c}_b,\, \mathbf{d},\, c) \in [\mathbb{B}_k(\partial K)]^2 \times \mathcal{G}_{k-2}(K)^\perp \times \mathbb{P}_{k-1}(K),$$

both satisfying the compatibility conditions, which correspond respectively to the couples $(\mathbf{v},\, s), (\mathbf{v},\, t) \in \mathbf{V}_h^K \times L^2(K)$ (*i.e.* same velocity and different pressures). Then it is straightforward to see that

$$\mathbf{g}_b = \mathbf{c}_b, \qquad g = c \qquad \text{and} \qquad \nabla(s-t) = \mathbf{d} - \mathbf{h}.$$

Therefore, we get $\mathrm{rot}(\mathbf{d} - \mathbf{h}) = 0$, where rot is the rotational operator in 2D, *i.e.* the rotated divergence. Since $\mathrm{rot}\colon \mathcal{G}_{k-2}(K)^\perp \to \mathbb{P}_{k-3}(K)$ is an isomorphism (see [11]), we conclude that $\mathbf{d} = \mathbf{h}$. Thus, there is an *injective* map $(\mathbf{g}_b,\, \mathbf{h},\, g) \to \mathbf{v}$ that associates a given compatible data set $(\mathbf{g}_b,\, \mathbf{h},\, g)$ to the velocity field $\mathbf{v}$ that solves (3.8). It follows that the dimension of $\mathbf{V}_h^K$ is

$$\begin{aligned} \dim\left(\mathbf{V}_h^K\right) &= \dim\left([\mathbb{B}_k(\partial K)]^2\right) + \dim\left(\mathcal{G}_{k-2}(K)^\perp\right) + \left(\dim(\mathbb{P}_{k-1}(K)) - 1\right) \\ &= 2n_K k + \frac{(k-1)(k-2)}{2} + \frac{(k+1)k}{2} - 1. \end{aligned} \tag{3.9}$$

For the local space Q_h^K we have

$$\dim(Q_h^K) = \dim(\mathbb{P}_{k-1}(K)) = \frac{(k+1)k}{2}\cdot \tag{3.10}$$

We are now ready to introduce suitable sets of degrees of freedom for the local approximation fields.

Given a function $\mathbf{v} \in \mathbf{V}_h^K$ we take the following linear operators $\mathbf{D_V}$, split into four subsets (see Fig. 1):

- $\mathbf{D_V 1}$: the values of $\mathbf{v}$ at the vertices of the polygon K,
- $\mathbf{D_V 2}$: the values of $\mathbf{v}$ at $k-1$ distinct points of every edge $e \in \partial K$ (for example we can take the $k-1$ internal points of the $(k+1)$-Gauss–Lobatto quadrature rule in e, as suggested in [9]),
- $\mathbf{D_V 3}$: the moments of $\mathbf{v}$

$$\int_K \mathbf{v} \cdot \mathbf{g}_{k-2}^\perp \,\mathrm{d}K \qquad \text{for all } \mathbf{g}_{k-2}^\perp \in \mathcal{G}_{k-2}(K)^\perp,$$

- $\mathbf{D_V 4}$: the moments up to order $k-1$ and greater than zero of $\operatorname{div} \mathbf{v}$ in K, *i.e.*

$$\int_K (\operatorname{div} \mathbf{v})\, q_{k-1} \,\mathrm{d}K \qquad \text{for all } q_{k-1} \in \mathbb{P}_{k-1}(K)/\mathbb{R}.$$

Furthermore, for the local pressure, given $q \in Q_h^K$, we consider the linear operators $\mathbf{D_Q}$:

- $\mathbf{D_Q}$: the moments up to order $k-1$ of q, *i.e.*

$$\int_K q\, p_{k-1} \,\mathrm{d}K \qquad \text{for all } p_{k-1} \in \mathbb{P}_{k-1}(K).$$

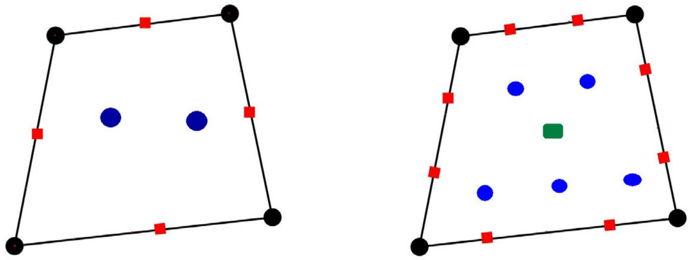

FIGURE 1. Degrees of freedom for $k = 2$, $k = 3$. We denote $\mathbf{D_V 1}$ with the black dots, $\mathbf{D_V 2}$ with the red squares, $\mathbf{D_V 3}$ with the green rectangles, $\mathbf{D_V 4}$ with the blued dots inside the elements. (Color online)

Since it is obvious that $\mathbf{D_Q}$ is unisolvent with respect to Q_h^K, it only remains to prove the unisolvence of $\mathbf{D_V}$. We first prove the following Lemma; we recall that all the differential operators are to be interpreted in the weak sense.

Lemma 3.1. *Let* $\mathbf{v} \in \mathbf{V}_h^K$ *such that* $\mathbf{D_V 1}(\mathbf{v}) = \mathbf{D_V 2}(\mathbf{v}) = \mathbf{D_V 4}(\mathbf{v}) = 0$. *Then*

$$\langle \nabla \varphi, \mathbf{v} \rangle_K = 0 \qquad \text{for all } \varphi \in L^2(K). \tag{3.11}$$

where, here and in the following, the brackets $\langle , \rangle_K$ *denote the duality pair between* $H_0^1(K)^2$ *and its dual* $H^{-1}(K)^2$.

Proof. It is clear that $\mathbf{D_V 1}(\mathbf{v}) = \mathbf{D_V 2}(\mathbf{v}) = 0$ implies $\mathbf{v}_{|\partial K} \equiv \mathbf{0}$. Therefore $\mathbf{v} \in H_0^1(K)$ and it holds

$$\langle \nabla \varphi, \mathbf{v} \rangle_K = -\int_K (\operatorname{div} \mathbf{v}) \varphi \, \mathrm{d}K.$$

Now, since $\mathbf{v} \in \mathbf{V}_h^K$, there exists $p_{k-1} \in \mathbb{P}_{k-1}(K)$ such that $\operatorname{div} \mathbf{v} = p_{k-1}$. Furthermore, by the divergence Theorem, we infer that $p_{k-1} \in \mathbb{P}_{k-1}(K)/\mathbb{R}$. Since $\mathbf{D_V 4}(\mathbf{v}) = 0$, we get:

$$\int_K (\operatorname{div} \mathbf{v})^2 \, \mathrm{d}K = \int_K \operatorname{div} \mathbf{v} \, p_{k-1} \, \mathrm{d}K = 0.$$

Therefore, $\operatorname{div} \mathbf{v} = 0$ and (3.11) follows. □

We now prove the following result.

Proposition 3.2. *The linear operators* $\mathbf{D_V}$ *are a unisolvent set of degrees of freedom for the virtual space* $\mathbf{V}_h^K$.

Proof. We start noting that the dimension of $\mathbf{V}_h^K$ equals the number of functionals in $\mathbf{D_V}$ and thus we only need to show that if all the values $\mathbf{D_V}(\mathbf{v})$ vanish for a given $\mathbf{v} \in \mathbf{V}_h^K$, then $\mathbf{v} = 0$. Since $\mathbf{D_V 1}(\mathbf{v}) = \mathbf{D_V 2}(\mathbf{v}) = 0$ implies $\mathbf{v} \equiv \mathbf{0}$ on ∂K, we have $\mathbf{v} \in H_0^1(K)$. Therefore

$$\int_K \nu \, \boldsymbol{\nabla} \mathbf{v} : \boldsymbol{\nabla} \mathbf{v} \, \mathrm{d}K = -\nu \langle \boldsymbol{\Delta} \mathbf{v}, \mathbf{v} \rangle_K.$$

Moreover, since $\mathbf{v} \in \mathbf{V}_h^K$, there exists a scalar function $s \in L^2(K)$ and $\mathbf{g}_{k-2}^{\perp} \in \mathcal{G}_{k-2}(K)^{\perp}$, such that

$$\nu \, \boldsymbol{\Delta} \mathbf{v} = -\nabla s - \mathbf{g}_{k-2}^{\perp} \quad \text{ in } H^{-1}(K)^2.$$

Then

$$\int_K \nu \, \boldsymbol{\nabla} \mathbf{v} : \boldsymbol{\nabla} \mathbf{v} \, \mathrm{d}K = \langle \nabla s, \mathbf{v} \rangle_K + \int_K \mathbf{g}_{k-2}^{\perp} \cdot \mathbf{v} \, \mathrm{d}K. \tag{3.12}$$

The first term at the right-hand side is zero from Lemma 3.1, while the second term vanishes because of the assumption $\mathbf{D_V 3}(\mathbf{v}) = 0$. Then $\mathbf{D_V}(\mathbf{v}) = 0$ implies $\mathbf{v} = 0$, and the proof is complete. □

We now define the global virtual element spaces as

$$\mathbf{V}_h := \{\mathbf{v} \in [H_0^1(\Omega)]^2 \quad \text{s.t} \quad \mathbf{v}_{|K} \in \mathbf{V}_h^K \quad \text{for all } K \in \mathcal{T}_h\} \tag{3.13}$$

and

$$Q_h := \{q \in L_0^2(\Omega) \quad \text{s.t.} \quad q_{|K} \in Q_h^K \quad \text{for all } K \in \mathcal{T}_h\}, \tag{3.14}$$

with the obvious associated sets of global degrees of freedom. A simple computation shows that it holds:

$$\dim(\mathbf{V}_h) = n_P \left(\frac{(k+1)k}{2} - 1 + \frac{(k-1)(k-2)}{2}\right) + 2(n_V + (k-1)n_E) \tag{3.15}$$

and

$$\dim(Q_h) = n_P \frac{(k+1)k}{2} - 1, \tag{3.16}$$

where n_P (resp., n_E and n_V) is the number of elements (resp., internal edges and vertexes) in $\mathcal{T}_h$.

We also remark that

$$\operatorname{div} \mathbf{V}_h \subseteq Q_h. \tag{3.17}$$

Remark 3.3. The space $\mathcal{G}_{k-2}(K)^{\perp}$ that defines the degrees of freedom $\boldsymbol{D_V 3}$ can be replaced by any space $\mathcal{G}_{k-2}(K)^{\oplus} \subseteq [\mathbb{P}_{k-2}(K)]^2$ that satisfies

$$[\mathbb{P}_{k-2}(K)]^2 = \mathcal{G}_{k-2}(K) \oplus \mathcal{G}_{k-2}(K)^{\oplus}.$$

An example is given by the space $\mathcal{G}_{k-2}(K)^{\oplus} := \mathbf{x}^{\perp}[\mathbb{P}_{k-3}(K)]^2$ with $\mathbf{x}^{\perp} := (x_2, -x_1)$.

Remark 3.4. We have built a new H^1-conforming (vector valued) virtual space for the velocity vector field, different from the more standard one presented in [8] for the elasticity problem. In fact, the original approach is to consider the local virtual space

$$\widetilde{\mathbf{V}}_h^K := \left\{\mathbf{v} \in [H^1(K)]^2 \quad \text{s.t} \quad \mathbf{v}_{|\partial K} \in [\mathbb{B}_k(\partial K)]^2, \quad \nu\, \boldsymbol{\Delta} \mathbf{v} \in [\mathbb{P}_{k-2}(K)]^2\right\} \tag{3.18}$$

with local degrees of freedom $\widetilde{\mathbf{D}}_{\mathbf{V}}$:

- $\widetilde{\mathbf{D}}_{\mathbf{V}}\mathbf{1}$: the values of $\mathbf{v}$ at each vertex of the polygon K,
- $\widetilde{\mathbf{D}}_{\mathbf{V}}\mathbf{2}$: the values of $\mathbf{v}$ at $k-1$ distinct points of every edge $e \in \partial K$,
- $\widetilde{\mathbf{D}}_{\mathbf{V}}\mathbf{3}$: the moments of $\mathbf{v}$ up to order $k-2$, *i.e.*

$$\int_K \mathbf{v} \cdot \mathbf{q}_{k-2} \, \mathrm{d}K \qquad \text{for all } \mathbf{q}_{k-2} \in [\mathbb{P}_{k-2}(K)]^2.$$

It can be easily checked that, for all k, the dimension of the spaces (3.4) and (3.18) are the same. On the other hand our local virtual space (3.4) is, in some sense, designed to solve a Stokes-like Problem element-wise, while the virtual space in (3.18) is designed to solve a classical Laplacian problem. As shown in the following, although both spaces can be used, the new choice (3.4) is better for the problem under consideration.

3.2. The discrete bilinear forms

We now define discrete versions of the bilinear form $a(\cdot,\cdot)$ (*cf.* (2.4)), and of the bilinear form $b(\cdot,\cdot)$ (*cf.* (2.5)). For what concerns $b(\cdot,\cdot)$, we simply set

$$b(\mathbf{v}, q) = \sum_{K \in \mathcal{T}_h} b^K(\mathbf{v}, q) = \sum_{K \in \mathcal{T}_h} \int_K \operatorname{div} \mathbf{v}\, q \, \mathrm{d}K \qquad \text{for all } \mathbf{v} \in \mathbf{V}_h,\ q \in Q_h, \tag{3.19}$$

i.e. we do not introduce any approximation of the bilinear form. We notice that (3.19) is computable from the degrees of freedom $\mathbf{D_V1}$, $\mathbf{D_V2}$ and $\mathbf{D_V4}$, since q is polynomial in each element $K \in \mathcal{T}_h$. The construction of a computable approximation of the bilinear form $a(\cdot,\cdot)$ on the virtual space $\mathbf{V}_h$ is more involved. First of all, we observe that $\forall\, \mathbf{q}_k \in [\mathbb{P}_k(K)]^2$ and $\forall\, \mathbf{v} \in \mathbf{V}_h^K$, the quantity $a^K(\mathbf{q}_k, \mathbf{v})$ is exactly computable. Indeed, we have

$$a^K(\mathbf{q}_k, \mathbf{v}) = \int_K \nu\, \boldsymbol{\nabla} \mathbf{q}_k : \boldsymbol{\nabla} \mathbf{v}\, \mathrm{d}K = -\int_K \nu\, \boldsymbol{\Delta} \mathbf{q}_k \cdot \mathbf{v}\, \mathrm{d}K + \int_{\partial K} (\nu\, \boldsymbol{\nabla} \mathbf{q}_k\, \mathbf{n}) \cdot \mathbf{v}\, \mathrm{d}s. \tag{3.20}$$

Since $\nu\, \boldsymbol{\Delta} \mathbf{q}_k \in [\mathbb{P}_{k-2}(K)]^2$, there exists a unique $q_{k-1} \in \mathbb{P}_{k-1}(K)/\mathbb{R}$ and $\mathbf{g}_{k-2}^{\perp} \in \mathcal{G}_{k-2}^{\perp}(K)$, such that

$$\nu\, \boldsymbol{\Delta} \mathbf{q}_k = \nabla q_{k-1} + \mathbf{g}_{k-2}^{\perp}. \tag{3.21}$$

Therefore, we get

$$\begin{aligned} a^K(\mathbf{q}_k, \mathbf{v}) &= -\int_K \nabla q_{k-1} \cdot \mathbf{v}\, \mathrm{d}K - \int_K \mathbf{g}_{k-2}^{\perp} \cdot \mathbf{v}\, \mathrm{d}K + \int_{\partial K} (\nu\, \boldsymbol{\nabla} \mathbf{q}_k\, \mathbf{n}) \cdot \mathbf{v}\, \mathrm{d}s \\ &= \int_K q_{k-1}\, \mathrm{div}\, \mathbf{v}\, \mathrm{d}K - \int_K \mathbf{g}_{k-2}^{\perp} \cdot \mathbf{v}\, \mathrm{d}K + \int_{\partial K} (\nu\, \boldsymbol{\nabla} \mathbf{q}_k\, \mathbf{n} - q_{k-1}\mathbf{n}) \cdot \mathbf{v}\, \mathrm{d}s. \end{aligned} \tag{3.22}$$

The first term in the right-hand side is computable from $\mathbf{D_V4}$, the second term from $\mathbf{D_V3}$ and the boundary term from $\mathbf{D_V1}$ and $\mathbf{D_V2}$. However, for an arbitrary pair $(\mathbf{w}, \mathbf{v}) \in \mathbf{V}_h^K \times \mathbf{V}_h^K$, the quantity $a_h^K(\mathbf{w}, \mathbf{v})$ is not computable. We now define a computable discrete local bilinear form

$$a_h^K(\cdot,\cdot)\colon \mathbf{V}_h^K \times \mathbf{V}_h^K \to \mathbb{R} \tag{3.23}$$

approximating the continuous form $a^K(\cdot,\cdot)$, and satisfying the following properties:

- **k-consistency**: for all $\mathbf{q}_k \in [\mathbb{P}_k(K)]^2$ and $\mathbf{v}_h \in \mathbf{V}_h^K$
$$a_h^K(\mathbf{q}_k, \mathbf{v}_h) = a^K(\mathbf{q}_k, \mathbf{v}_h); \tag{3.24}$$
- **stability**: there exist two positive constants α_* and α^*, independent of h and K, such that, for all $\mathbf{v}_h \in \mathbf{V}_h^K$, it holds
$$\alpha_* a^K(\mathbf{v}_h, \mathbf{v}_h) \leq a_h^K(\mathbf{v}_h, \mathbf{v}_h) \leq \alpha^* a^K(\mathbf{v}_h, \mathbf{v}_h). \tag{3.25}$$

For all $K \in \mathcal{T}_h$, we introduce the energy projection operator $\Pi_k^{\nabla,K}\colon \mathbf{V}_h^K \to [\mathbb{P}_k(K)]^2$, defined by

$$\begin{cases} a^K(\mathbf{q}_k, \mathbf{v}_h - \Pi_k^{\nabla,K} \mathbf{v}_h) = 0 & \text{for all } \mathbf{q}_k \in [\mathbb{P}_k(K)]^2, \\ P^{0,K}(\mathbf{v}_h - \Pi_k^{\nabla,K} \mathbf{v}_h) = \mathbf{0}, \end{cases} \tag{3.26}$$

where $P^{0,K}$ is the L^2-projection operator onto the constant functions defined on K. It is immediate to check that the energy projection is well defined. Moreover, it clearly holds $\Pi_k^{\nabla,K} \mathbf{q}_k = \mathbf{q}_k$ for all $\mathbf{q}_k \in \mathbb{P}_k(K)$.

Remark 3.5. Since $a^K(\mathbf{q}_k, \mathbf{v}_h)$ is computable (see Eq. (3.22) and the subsequent discussion), it follows that the operator $\Pi_k^{\nabla,K}$ is computable in terms of the degrees of freedom $\mathbf{D_V}$ as well.

As usual in the VEM framework, we now introduce a (symmetric) stabilizing bilinear form $\mathcal{S}^K\colon \mathbf{V}_h^K \times \mathbf{V}_h^K \to \mathbb{R}$, that satisfies

$$c_* a^K(\mathbf{v}_h, \mathbf{v}_h) \leq \mathcal{S}^K(\mathbf{v}_h, \mathbf{v}_h) \leq c^* a^K(\mathbf{v}_h, \mathbf{v}_h) \qquad \text{for all } \mathbf{v}_h \in \mathbf{V}_h \text{ such that } \Pi_k^{\nabla,K} \mathbf{v}_h = \mathbf{0}. \tag{3.27}$$

Above, c_* and c^* are two positive constants, independent of h and K.

Then, we can set

$$a_h^K(\mathbf{u}_h, \mathbf{v}_h) := a^K\left(\Pi_k^{\nabla,K}\mathbf{u}_h, \Pi_k^{\nabla,K}\mathbf{v}_h\right) + \mathcal{S}^K\left((I - \Pi_k^{\nabla,K})\mathbf{u}_h, (I - \Pi_k^{\nabla,K})\mathbf{v}_h\right) \tag{3.28}$$

for all $\mathbf{u}_h, \mathbf{v}_h \in \mathbf{V}_h^K$.

It is easy to see that Definition (3.26) and estimates (3.27) imply the consistency and the stability of the bilinear form $a_h^K(\cdot,\cdot)$.

Remark 3.6. Condition (3.27) essentially states that the stabilizing term $\mathcal{S}^K(\mathbf{v}_h, \mathbf{v}_h)$ scales as $a^K(\mathbf{v}_h, \mathbf{v}_h)$. We briefly sketch an example of this construction, that follows a standard VEM technique (*cf.* [7,9] for more details). Let us denote with $\bar{\mathbf{v}}_h$, $\bar{\mathbf{w}}_h \in \mathbb{R}^{N_K}$ the vectors containing the values of the N_K local degrees of freedom associated to $\mathbf{v}_h, \mathbf{w}_h \in \mathbf{V}_h^K$. Then, we set

$$\mathcal{S}^K(\mathbf{v}_h, \mathbf{w}_h) = \alpha^K\, \bar{\mathbf{v}}_h^T \bar{\mathbf{w}}_h,$$

where α^K is a suitable positive constant independent of the element size. For example, in the numerical tests presented in Section 6, we have chosen α^K as the mean value of the eigenvalues of the matrix stemming from the term $a^K\left(\Pi_k^{\nabla,K}\mathbf{v}_h, \Pi_k^{\nabla,K}\mathbf{w}_h\right)$, see (3.28).

Finally we define the global approximated bilinear form $a_h(\cdot,\cdot)\colon \mathbf{V}_h \times \mathbf{V}_h \to \mathbb{R}$ by simply summing the local contributions:

$$a_h(\mathbf{u}_h, \mathbf{v}_h) := \sum_{K \in \mathcal{T}_h} a_h^K(\mathbf{u}_h, \mathbf{v}_h) \qquad \text{for all } \mathbf{u}_h, \mathbf{v}_h \in \mathbf{V}_h. \tag{3.29}$$

3.3. Load term approximation

The last step consists in constructing a computable approximation of the right-hand side $(\mathbf{f}, \mathbf{v})$ in (2.6). Let $K \in \mathcal{T}_h$, and let $\Pi_{k-2}^{0,K}\colon [L^2(K)]^2 \to [\mathbb{P}_{k-2}(K)]^2$ be the $L^2(K)$ projection operator onto the space $[\mathbb{P}_{k-2}(K)]^2$. Then, we define the approximated load term $\mathbf{f}_h$ as

$$\mathbf{f}_h := \Pi_{k-2}^{0,K}\mathbf{f} \qquad \text{for all } K \in \mathcal{T}_h, \tag{3.30}$$

and consider:

$$(\mathbf{f}_h, \mathbf{v}_h) = \sum_{K \in \mathcal{T}_h} \int_K \mathbf{f}_h \cdot \mathbf{v}_h \,\mathrm{d}K = \sum_{K \in \mathcal{T}_h} \int_K \Pi_{k-2}^{0,K}\mathbf{f} \cdot \mathbf{v}_h \,\mathrm{d}K = \sum_{K \in \mathcal{T}_h} \int_K \mathbf{f} \cdot \Pi_{k-2}^{0,K}\mathbf{v}_h \,\mathrm{d}K. \tag{3.31}$$

We observe that (3.31) can be exactly computed for all $\mathbf{v}_h \in \mathbf{V}_h$. In fact, $\Pi_{k-2}^{0,K}\mathbf{v}_h$ is computable in terms of the degrees of freedom $\mathbf{D_V}$: for all $\mathbf{q}_{k-2} \in [\mathbb{P}_{k-2}(K)]^2$ we have

$$\int_K \Pi_{k-2}^{0,K}\mathbf{v}_h \cdot \mathbf{q}_{k-2} \,\mathrm{d}K = \int_K \mathbf{v}_h \cdot \mathbf{q}_{k-2} \,\mathrm{d}K = \int_K \mathbf{v}_h \cdot \nabla q_{k-1} \,\mathrm{d}K + \int_K \mathbf{v}_h \cdot \mathbf{g}_{k-2}^{\perp} \,\mathrm{d}K$$

for suitable $q_{k-1} \in \mathbb{P}_{k-1}(K)$ and $\mathbf{g}_{k-2}^{\perp} \in \mathcal{G}_{k-2}(K)^{\perp}$. As a consequence, we get

$$\int_K \Pi_{k-2}^{0,K}\mathbf{v}_h \cdot \mathbf{q}_{k-2} \,\mathrm{d}K = -\int_K \operatorname{div}\mathbf{v}_h\, q_{k-1} \,\mathrm{d}K + \int_{\partial K} q_{k-1}\mathbf{v}_h \cdot \mathbf{n} \,\mathrm{d}s + \int_K \mathbf{v}_h \cdot \mathbf{g}_{k-2}^{\perp} \,\mathrm{d}K,$$

and the right-hand side is directly computable from $\mathbf{D_V}$.

Furthermore, the following result concerning a H^{-1}-type norm, can be proved using standard arguments [7].

Lemma 3.7. *Let $\mathbf{f}_h$ be defined as in (3.30), and let us assume $\mathbf{f} \in H^{k-1}(\Omega)$. Then, for all $\mathbf{v}_h \in \mathbf{V}_h$, it holds*

$$|(\mathbf{f}_h - \mathbf{f}, \mathbf{v}_h)| \le C h^k |\mathbf{f}|_{k-1} \|\mathbf{v}_h\|_1.$$

3.4. The discrete problem

We are now ready to state the proposed discrete problem. Referring to (3.19), (3.29) and (3.30)–(3.31), we consider the virtual element problem:

$$\begin{cases} \text{find } (\mathbf{u}_h, p_h) \in \mathbf{V}_h \times Q_h, \text{ such that} \\ a_h(\mathbf{u}_h, \mathbf{v}_h) + b(\mathbf{v}_h, p_h) = (\mathbf{f}_h, \mathbf{v}_h) & \text{for all } \mathbf{v}_h \in \mathbf{V}_h, \\ b(\mathbf{u}_h, q_h) = 0 & \text{for all } q_h \in Q_h. \end{cases} \tag{3.32}$$

By construction (see (3.25), (3.27) and (3.28)) the discrete bilinear form $a_h(\cdot,\cdot)$ is (uniformly) stable with respect to the $\mathbf{V}$ norm. Therefore, the existence and the uniqueness of the solution to problem (3.32) will follow if a suitable inf-sup condition is fulfilled, which is the topic of Section 4.1.

We also remark that the second equation of (3.32), along with property (3.17), implies that the discrete velocity $\mathbf{u}_h \in \mathbf{V}_h$ is *exactly divergence-free*. More generally, introducing the kernels:

$$\mathbf{Z} := \{\mathbf{v} \in \mathbf{V} \quad \text{s.t.} \quad b(\mathbf{v}, q) = 0 \quad \text{for all } q \in Q\} \tag{3.33}$$

and

$$\mathbf{Z}_h := \{\mathbf{v}_h \in \mathbf{V}_h \quad \text{s.t.} \quad b(\mathbf{v}_h, q_h) = 0 \quad \text{for all } q_h \in Q_h\}, \tag{3.34}$$

it is immediate to check that

$$\mathbf{Z}_h \subseteq \mathbf{Z}. \tag{3.35}$$

Remark 3.8. The method presented in this paper differs from the one studied in [8]. Indeed, the former scheme leads to a discrete velocity solution which is *exactly divergence-free* (for every k, and every polytopal mesh), while the latter leads to a discrete velocity solution which is divergence-free *only weakly*. Moreover, the numerical results presented in Section 6 confirm that the two schemes are not equivalent.

Remark 3.9. We remark that our method, when using triangular or quadrilateral meshes, is different from already-known finite element schemes. Focusing on the case $k = 2$ and triangular meshes, we now briefly compare our VEM approach with the mixed finite element scheme employing the approximation couple $(\mathbf{V}_h^{FEM}, Q_h)$, where

$$\mathbf{V}_h^{FEM} := \{\mathbf{v}_h \in \mathbf{V} : \ \mathbf{v}_{h|K} \in [\mathbb{P}_3(K) \cap \mathbb{B}_2(\partial K)]^2, \quad \forall K \in \mathcal{T}_h\}. \tag{3.36}$$

The above choice could be seen as a discontinuous pressure version of the lowest-order Hood–Taylor element, stabilized by means of cubic bubble functions. We notice that $\dim(\mathbf{V}_h) = \dim(\mathbf{V}_h^{FEM})$, and that $[\mathbb{P}_2(K)]^2 \subset \mathbf{V}_h \cap \mathbf{V}_h^{FEM}$ for every $K \in \mathcal{T}_h$. Therefore, one could be tempted to infer that the two methods coincide. However, for the VEM scheme it holds $\operatorname{div} \mathbf{V}_h \subseteq Q_h$ (in fact: $\operatorname{div} \mathbf{V}_h = Q_h$, *cf.* (3.8)), while for the FEM scheme it holds $\operatorname{div} \mathbf{V}_h \not\subseteq Q_h$, because the divergence of a cubic bubble function is not a linear polynomial. This argument shows that the two approaches are indeed different. Similar considerations apply for quadrilateral meshes and for general k, in connection with the corresponding stabilized Hood–Taylor element using discontinuous pressure.

4. Theoretical results

We begin by proving an approximation result for the virtual local space $\mathbf{V}_h$. First of all, let us recall a classical result by Brenner–Scott (see [18]).

Lemma 4.1. *Let $K \in \mathcal{T}_h$, then for all $\mathbf{u} \in [H^{s+1}(K)]^2$ with $0 \le s \le k$, there exists a polynomial function $\mathbf{u}_\pi \in [\mathbb{P}_k(K)]^2$, such that*

$$\|\mathbf{u} - \mathbf{u}_\pi\|_{0,K} + h_K |\mathbf{u} - \mathbf{u}_\pi|_{1,K} \le C h_K^{s+1} |\mathbf{u}|_{s+1,K}. \tag{4.1}$$

We have the following proposition.

Proposition 4.2. *Let $\mathbf{u} \in \mathbf{V} \cap [H^{s+1}(\Omega)]^2$ with $0 \le s \le k$. Under the assumption* (**A1**) *and* (**A2**) *on the decomposition $\mathcal{T}_h$, there exists $\mathbf{u}_I \in \mathbf{V}_h$ such that*

$$\|\mathbf{u} - \mathbf{u}_I\|_{0,K} + h_K |\mathbf{u} - \mathbf{u}_I|_{1,K} \le C h_K^{s+1} |\mathbf{u}|_{s+1,D(K)} \tag{4.2}$$

where C is a constant independent of h, and $D(K)$ denotes the "diamond" of K, i.e. *the union of the polygons in $\mathcal{T}_h$ intersecting K.*

Proof. The proof follows the guidelines of Proposition 4.2 in [40]. For each polygon $K \in \mathcal{T}_h$, let us consider the triangulation $\mathcal{T}_h^K$ of K obtained by joining each vertex of K with the center of the ball with respect to which K is star-shaped. Set now $\widehat{\mathcal{T}}_h := \bigcup_{K \in \mathcal{T}_h} \mathcal{T}_h^K$, which is a triangular decomposition of the domain Ω.

Let $\mathbf{u}_c$ be the Clément interpolant of order k of the function $\mathbf{u}$, relative to the triangular decomposition $\widehat{\mathcal{T}}_h$ (see [26]). Then $\mathbf{u}_c \in [H^1(\Omega)]^2$ and it holds

$$\|\mathbf{u} - \mathbf{u}_c\|_{0,K} + h_K |\mathbf{u} - \mathbf{u}_c|_{1,K} \le C h_K^{s+1} |\mathbf{u}|_{s+1,D(K)}. \tag{4.3}$$

Let, for each polygon K, $\mathbf{u}_\pi$ be the polynomial approximation of $\mathbf{u}$ as in Lemma 4.1. Then we have:

$$\nu\, \Delta \mathbf{u}_\pi = \nabla p_\pi + \mathbf{g}_\pi^\perp, \tag{4.4}$$

for suitable $p_\pi \in \mathbb{P}_{k-1}(K)$ and $\mathbf{g}_\pi^\perp \in \mathcal{G}_{k-2}(K)^\perp$. Let $p_c := \Pi_{k-1}^{0,K}(\operatorname{div} \mathbf{u}_c)$ for all $K \in \mathcal{T}_h$. We introduce the following local Stokes problem

$$\begin{cases} -\nu\, \boldsymbol{\Delta} \mathbf{u}_I - \nabla s = -\mathbf{g}_\pi^\perp & \text{in } K, \\ \operatorname{div} \mathbf{u}_I = p_c & \text{in } K, \\ \mathbf{u}_I = \mathbf{u}_c & \text{on } \partial K. \end{cases} \tag{4.5}$$

It is straightforward to check that $\mathbf{u}_I \in \mathbf{V}_h^K$. Furthermore, since $\mathbf{u}_I = \mathbf{u}_c$ on each boundary ∂K, $\mathbf{u}_I \in [H^1(\Omega)]^2$. We infer that $\mathbf{u}_I \in \mathbf{V}_h$. We now prove that $\mathbf{u}_I$ satisfies estimate (4.2). We consider the following auxiliary local Stokes problem

$$\begin{cases} -\nu\, \boldsymbol{\Delta}\, \widetilde{\mathbf{u}} - \nabla \widetilde{s} = -\mathbf{g}_\pi^\perp & \text{in } K, \\ \operatorname{div} \widetilde{\mathbf{u}} = \operatorname{div} \mathbf{u}_c & \text{in } K, \\ \widetilde{\mathbf{u}} = \mathbf{u}_c & \text{on } \partial K. \end{cases} \tag{4.6}$$

By (4.6) and (4.4), we get

$$\begin{cases} -\nu\, \boldsymbol{\Delta}(\mathbf{u}_\pi - \widetilde{\mathbf{u}}) - \nabla(-p_\pi - \widetilde{s}) = \mathbf{0} & \text{in } K, \\ \operatorname{div}\, (\mathbf{u}_\pi - \widetilde{\mathbf{u}}) = \operatorname{div}\, (\mathbf{u}_\pi - \mathbf{u}_c) & \text{in } K, \\ \mathbf{u}_\pi - \widetilde{\mathbf{u}} = \mathbf{u}_\pi - \mathbf{u}_c & \text{on } \partial K. \end{cases} \tag{4.7}$$

Therefore we get

$$|\mathbf{u}_\pi - \widetilde{\mathbf{u}}|_{1,K} = \inf\{|\mathbf{z}|_{1,K} : \mathbf{z} \in [H^1(K)]^2,\ \operatorname{div} \mathbf{z} = \operatorname{div}\, (\mathbf{u}_\pi - \mathbf{u}_c) \text{ and } \mathbf{z} = \mathbf{u}_\pi - \mathbf{u}_c \text{ on } \partial K\}.$$

Choosing $\mathbf{z} = \mathbf{u}_\pi - \mathbf{u}_c$, by Lemma 4.1 and estimates (4.1) and (4.3), we obtain

$$|\mathbf{u}_\pi - \widetilde{\mathbf{u}}|_{1,K} \le |\mathbf{u}_\pi - \mathbf{u}_c|_{1,K} \le |\mathbf{u}_\pi - \mathbf{u}|_{1,K} + |\mathbf{u} - \mathbf{u}_c|_{1,K} \le C\, h_K^s |\mathbf{u}|_{s+1,D(K)}. \tag{4.8}$$

Subtracting (4.5) from (4.6), we have

$$\begin{cases} -\nu\, \boldsymbol{\Delta}(\widetilde{\mathbf{u}} - \mathbf{u}_I) - \nabla(\widetilde{s} - s) = \mathbf{0} & \text{in } K, \\ \operatorname{div}\, (\widetilde{\mathbf{u}} - \mathbf{u}_I) = \operatorname{div} \mathbf{u}_c - p_c & \text{in } K, \\ \widetilde{\mathbf{u}} - \mathbf{u}_I = \mathbf{0} & \text{on } \partial K. \end{cases}$$

Using the standard theory of saddle point problems (see for instance [16]), we get

$$|\widetilde{\mathbf{u}} - \mathbf{u}_I|_{1,K} \leq \frac{1}{\beta(K)}\left(1 + \frac{\|a^K\|}{\alpha^K}\right)\|\operatorname{div}\mathbf{u}_c - p_c\|_{0,K}$$

where $\beta(K)$ is the inf-sup constant on the polygon K (*cf.* (2.7)) and $\|a^K\|$ and α^K denote respectively the norm and the coercivity constant of $a^K(\cdot,\cdot)$. It is straightforward to check that

$$\|a^K\| = \nu \qquad \text{and} \qquad \alpha^K \geq \frac{\nu}{1+h_K^2}\cdot$$

Therefore, recalling that $p_c := \Pi_{k-1}^{0,K}(\operatorname{div}\mathbf{u}_c)$, using first the triangle inequality, then estimate (4.3) and standard estimates, we have

$$\begin{aligned}
|\widetilde{\mathbf{u}} - \mathbf{u}_I|_{1,K} &\leq \frac{2+h_K^2}{\beta(K)}\left(\left\|(I-\Pi_{k-1}^{0,K})\left(\operatorname{div}\mathbf{u} - \operatorname{div}\mathbf{u}_c\right)\right\|_{0,K} + \left\|(I-\Pi_{k-1}^{0,K})\operatorname{div}\mathbf{u}\right\|_{0,K}\right)\\
&\leq \frac{C}{\beta(K)}\left(\|\operatorname{div}(\mathbf{u}-\mathbf{u}_c)\|_{0,K} + h_K^s|\operatorname{div}\mathbf{u}|_{s,K}\right)\\
&\leq \frac{C}{\beta(K)}\left(|\mathbf{u}-\mathbf{u}_c|_{1,K} + h_K^s|\mathbf{u}|_{s+1,K}\right) \leq \frac{C}{\beta(K)}\,h_K^s|\mathbf{u}|_{s+1,D(K)}.
\end{aligned}$$

By assumption (**A1**) and using the results in [30, 32], the inf-sup constant $\beta(K)$ is uniformly bounded from below: there exists $c > 0$, independent of h, such that $\beta(K) \geq c$ for all $K \in \mathcal{T}_h$. Therefore, it holds

$$|\widetilde{\mathbf{u}} - \mathbf{u}_I|_{1,K} \leq C\,h_K^s|\mathbf{u}|_{s+1,D(K)}. \tag{4.9}$$

The triangle inequality together with estimates (4.1), (4.8) and (4.9), give

$$|\mathbf{u}-\mathbf{u}_I|_{1,K} \leq |\mathbf{u}-\mathbf{u}_\pi|_{1,K} + |\mathbf{u}_\pi - \widetilde{\mathbf{u}}|_{1,K} + |\widetilde{\mathbf{u}} - \mathbf{u}_I|_{1,K} \leq Ch_K^s|\mathbf{u}|_{s+1,D(K)} \tag{4.10}$$

Furthermore, for each polygon $K \in \mathcal{T}_h$, we have that $\mathbf{u}_I - \mathbf{u}_c = \mathbf{0}$ on ∂K, see (4.5). Hence, it holds

$$\|\mathbf{u}_I - \mathbf{u}_c\|_{0,K} \leq C\,h_K|\mathbf{u}_I - \mathbf{u}_c|_{1,K}.$$

Therefore, we get

$$\begin{aligned}
\|\mathbf{u}-\mathbf{u}_I\|_{0,K} &\leq \|\mathbf{u}-\mathbf{u}_c\|_{0,K} + \|\mathbf{u}_c - \mathbf{u}_I\|_{0,K} \leq C\left(h_K^{s+1}|\mathbf{u}|_{s+1,D(K)} + h_K|\mathbf{u}_I - \mathbf{u}_c|_{1,K}\right)\\
&\leq \left(h_K^{s+1}|\mathbf{u}|_{s+1,D(K)} + h_K|\mathbf{u}-\mathbf{u}_I|_{1,K} + h_K|\mathbf{u}-\mathbf{u}_c|_{1,K}\right) \leq C\,h_K^{s+1}|\mathbf{u}|_{s+1,D(K)}.
\end{aligned} \tag{4.11}$$

From (4.10) and (4.11), we infer estimate (4.2). □

4.1. A stability result: The inf-sup condition

The aim of this section is to prove that the following inf-sup condition holds.

Proposition 4.3. *Given the discrete spaces $\mathbf{V}_h$ and Q_h defined in (3.13) and (3.14), there exists a positive $\tilde{\beta}$, independent of h, such that:*

$$\sup_{\mathbf{v}_h\in\mathbf{V}_h\,\mathbf{v}_h\neq\mathbf{0}} \frac{b(\mathbf{v}_h, q_h)}{\|\mathbf{v}_h\|_1} \geq \tilde{\beta}\|q_h\|_Q \qquad \textit{for all } q_h \in Q_h. \tag{4.12}$$

Proof. We only sketch the proof, because it essentially follows the guidelines of Theorem 3.1 in [8]. Since the continuous inf-sup condition (2.7) is fulfilled, it is sufficient to construct a linear operator $\pi_h : \mathbf{V} \to \mathbf{V}_h$, satisfying (see [16]):

$$\begin{cases} b(\pi_h \mathbf{v}, q_h) = b(\mathbf{v}, q_h) & \forall\, \mathbf{v} \in \mathbf{V}, \forall\, q_h \in Q_h, \\ \|\pi_h \mathbf{v}\|_1 \le c_\pi \|\mathbf{v}\|_1 & \forall\, \mathbf{v} \in \mathbf{V}, \end{cases} \tag{4.13}$$

where c_π is a positive h-independent constant. Given $\mathbf{v} \in \mathbf{V}$, recalling that $k \ge 2$ ($cf.$ (3.4)), using arguments borrowed from [8], and considering the VEM interpolant $\mathbf{v}_I$ presented in Proposition 4.2, we first construct $\bar{\mathbf{v}}_h \in \mathbf{V}_h$ such that

$$b(\mathbf{v} - \bar{\mathbf{v}}_h, \bar{q}_h) = 0 \qquad \forall\, \bar{q}_h \text{ piecewise constant function in } \mathcal{T}_h$$

and

$$\|\mathbf{v} - \bar{\mathbf{v}}_h\|_1 \le C \|\mathbf{v}\|_1 \qquad \forall\, \mathbf{v} \in \mathbf{V}. \tag{4.14}$$

Next, we build a "bubble" function $\widetilde{\mathbf{v}}_h \in \mathbf{V}_h$, locally defined as follows. Given $K \in \mathcal{T}_h$, we set all the degrees of freedom $\mathbf{D_V1}$, $\mathbf{D_V2}$ and $\mathbf{D_V3}$ equal to zero, while we set the degrees of freedom $\mathbf{D_V4}$ imposing

$$b^K(\widetilde{\mathbf{v}}_h, q_k) = b^K(\mathbf{v} - \bar{\mathbf{v}}_h, q_k) \qquad \forall\, q_k \in \mathbb{P}_{k-1}(K). \tag{4.15}$$

It holds:

$$\|\widetilde{\mathbf{v}}_h\|_1 \le C \|\mathbf{v} - \bar{\mathbf{v}}_h\|_1 \le C \|\mathbf{v}\|_1. \tag{4.16}$$

Now we set

$$\pi_h \mathbf{v} := \bar{\mathbf{v}}_h + \widetilde{\mathbf{v}}_h \qquad \text{for all } \mathbf{v} \in \mathbf{V}.$$

By (4.15), we have

$$b(\mathbf{v} - \pi_h \mathbf{v}, q_h) = b(\mathbf{v} - \bar{\mathbf{v}}_h, q_h) - b(\widetilde{\mathbf{v}}_h, q_h) = 0 \qquad \text{for all } q_h \in Q_h,$$

and combining (4.14) and (4.16), we get

$$\|\pi_h \mathbf{v}\|_1 = \|\bar{\mathbf{v}}_h + \widetilde{\mathbf{v}}_h\|_1 \le \|\bar{\mathbf{v}}_h - \mathbf{v}\|_1 + \|\mathbf{v}\|_1 + \|\widetilde{\mathbf{v}}_h\|_1 \le C \|\mathbf{v}\|_1.$$ □

An immediate consequence of the previous result is the following Theorem.

Theorem 4.4. *Problem* (3.32) *has a unique solution* $(\mathbf{u}_h, p_h) \in \mathbf{V}_h \times Q_h$, *verifying the estimate*

$$\|\mathbf{u}_h\|_1 + \|p_h\|_Q \le C \|\mathbf{f}\|_0.$$

Moreover, the inf-sup condition of Proposition 4.3, along with property (3.17), implies that:

$$\operatorname{div} \mathbf{V}_h = Q_h. \tag{4.17}$$

Remark 4.5. An analogous result of Proposition 4.3 is shown in [8], where the discrete inf-sup condition is detailed for the virtual local spaces defined in Remark 3.4. Therefore, as already observed, also the spaces of [8] could be directly used as a stable pair for the Stokes problem. On the other hand, the choice in [8] would not satisfy condition (3.35) and thus the discrete solution would not be divergence free. Moreover, such spaces would not share the interesting property to be equivalent to a suitable reduced problem ($cf.$ Sect. 5).

4.2. A convergence result

We begin by remarking that, using Proposition 4.2 and classical approximation theory, for $\mathbf{v} \in [H^{k+1}(\Omega)]^2$ and $q \in H^k(\Omega)$ it holds

$$\inf_{\mathbf{v}_h \in \mathbf{V}_h} \|\mathbf{v} - \mathbf{v}_h\|_1 \leq C h^k |\mathbf{v}|_{k+1} \tag{4.18}$$

and

$$\inf_{\mathbf{q}_h \in \mathbf{Q}_h} \|q - q_h\|_Q \leq C h^k |q|_k. \tag{4.19}$$

We now notice that, if $\mathbf{u} \in \mathbf{V}$ is the velocity solution to problem (2.6), then it is the solution to problem (*cf.* also (3.33)):

$$\begin{cases} \text{find } \mathbf{u} \in \mathbf{Z} \\ a(\mathbf{u}, \mathbf{v}) = (\mathbf{f}, \mathbf{v}) \qquad \text{for all } \mathbf{v} \in \mathbf{Z}. \end{cases} \tag{4.20}$$

Analogously, if $\mathbf{u}_h \in \mathbf{V}_h$ is the velocity solution to problem (3.32), then it is the solution to Problem (*cf.* also (3.34)):

$$\begin{cases} \text{find } \mathbf{u}_h \in \mathbf{Z}_h \\ a_h(\mathbf{u}_h, \mathbf{v}_h) = (\mathbf{f}_h, \mathbf{v}_h) \qquad \text{for all } \mathbf{v}_h \in \mathbf{Z}_h, \end{cases} \tag{4.21}$$

Recalling (3.35), problem (4.21) can be seen as a standard virtual approximation of the elliptic problem (4.20). Furthermore, given $\mathbf{z} \in \mathbf{Z}$, the inf-sup condition (4.12) implies (see for instance the book [16], Prop. 5.1.3, p. 273):

$$\inf_{\mathbf{z}_h \in \mathbf{Z}_h} ||\mathbf{z} - \mathbf{z}_h||_1 \leq C \inf_{\mathbf{v}_h \in \mathbf{V}_h} ||\mathbf{z} - \mathbf{v}_h||_1,$$

which essentially means that $\mathbf{Z}$ is approximated by $\mathbf{Z}_h$ with the same accuracy order of the whole subspace $\mathbf{V}_h$. As a consequence, usual VEM arguments (for instance, as in [7]) and (4.18) lead to the following result.

Theorem 4.6. *Let $\mathbf{u} \in \mathbf{Z}$ be the solution of problem (4.20) and $\mathbf{u}_h \in \mathbf{Z}_h$ be the solution of problem (4.21). Then*

$$\|\mathbf{u} - \mathbf{u}_h\|_1 \leq C h^k \left(|\mathbf{f}|_{k-1} + |\mathbf{u}|_{k+1}\right).$$

We proceed by analysing the error on the pressure field. We are ready to prove the following error estimates for the pressure approximation.

Theorem 4.7. *Let $(\mathbf{u}, p) \in \mathbf{V} \times Q$ be the solution of problem (2.6) and $(\mathbf{u}_h, p_h) \in \mathbf{V}_h \times Q_h$ be the solution of problem (3.32). Then it holds:*

$$\|p - p_h\|_Q \leq C h^k \left(|\mathbf{f}|_{k-1} + |\mathbf{u}|_{k+1} + |p|_k\right). \tag{4.22}$$

Proof. Let $q_h \in Q_h$. From the discrete inf-sup condition (4.12), we infer:

$$\tilde{\beta} \|p_h - q_h\|_Q \leq \sup_{\mathbf{v}_h \in \mathbf{V}_h \, \mathbf{v}_h \neq \mathbf{0}} \frac{b(\mathbf{v}_h, p_h - q_h)}{\|\mathbf{v}_h\|_1} = \sup_{\mathbf{v}_h \in \mathbf{V}_h \, \mathbf{v}_h \neq \mathbf{0}} \frac{b(\mathbf{v}_h, p_h - p) + b(\mathbf{v}_h, p - q_h)}{\|\mathbf{v}_h\|_1}. \tag{4.23}$$

Since $(\mathbf{u}, p)$ and $(\mathbf{u}_h, p_h)$ are the solution of (2.6) and (3.32), respectively, it follows that

$$\begin{aligned} a(\mathbf{u}, \mathbf{v}_h) + b(\mathbf{v}_h, p) &= (\mathbf{f}, \mathbf{v}_h) \qquad \text{for all } \mathbf{v}_h \in \mathbf{V}_h, \\ a_h(\mathbf{u}_h, \mathbf{v}_h) + b(\mathbf{v}_h, p_h) &= (\mathbf{f}_h, \mathbf{v}_h) \qquad \text{for all } \mathbf{v}_h \in \mathbf{V}_h. \end{aligned}$$

Therefore, we get

$$b(\mathbf{v}_h, p_h - p) = (\mathbf{f}_h - \mathbf{f}, \mathbf{v}_h) + (a(\mathbf{u}, \mathbf{v}_h) - a_h(\mathbf{u}_h, \mathbf{v}_h)) =: \mu_1(\mathbf{v}_h) + \mu_2(\mathbf{v}_h) \qquad \text{for all } \mathbf{v}_h \in \mathbf{V}_h. \tag{4.24}$$

The term $\mu_1(\mathbf{v}_h)$ can be bounded by making use of Lemma 3.7:

$$|\mu_1(\mathbf{v}_h)| \leq Ch^k |\mathbf{f}|_{k-1} \|\mathbf{v}_h\|_1. \tag{4.25}$$

For the term $\mu_2(\mathbf{v}_h)$, using (3.24) and the continuity of $a_h(\cdot,\cdot)$ and the triangle inequality, we get:

$$\begin{aligned}
\mu_2(\mathbf{v}_h) = a(\mathbf{u}, \mathbf{v}_h) - a_h(\mathbf{u}_h, \mathbf{v}_h) &= \sum_{K \in \mathcal{T}_h} \left(a^K(\mathbf{u}, \mathbf{v}_h) - a_h^K(\mathbf{u}_h, \mathbf{v}_h) \right) \\
&= \sum_{K \in \mathcal{T}_h} \left(a^K(\mathbf{u} - \mathbf{u}_\pi, \mathbf{v}_h) + a_h^K(\mathbf{u}_\pi - \mathbf{u}_h, \mathbf{v}_h) \right) \\
&\leq \sum_{K \in \mathcal{T}_h} C \big(|\mathbf{u} - \mathbf{u}_\pi|_{1,K} + |(\mathbf{u}_\pi - \mathbf{u}_h) \big) |\mathbf{v}_h|_{1,K} \\
&\leq \sum_{K \in \mathcal{T}_h} C \big(|\mathbf{u} - \mathbf{u}_\pi|_{1,K} + |\mathbf{u} - \mathbf{u}_h|_{1,K} \big) |\mathbf{v}_h|_{1,K}
\end{aligned}$$

where $\mathbf{u}_\pi$ is the piecewise polynomial of degree k defined in Lemma 4.1. Then, from estimate (4.1) and Theorem 4.6, we obtain

$$|\mu_2(\mathbf{v}_h)| \leq Ch^k \left(|\mathbf{f}|_{k-1} + |\mathbf{u}|_{k+1} \right) \|\mathbf{v}_h\|_1. \tag{4.26}$$

Then, combining (4.25) and (4.26) in (4.24), we get

$$|b(\mathbf{v}_h, p_h - p)| \leq Ch^k \left(|\mathbf{f}|_{k-1} + |\mathbf{u}|_{k+1} \right) \|\mathbf{v}_h\|_1. \tag{4.27}$$

Moreover, we have

$$|b(\mathbf{v}_h, p - q_h)| \leq C \|p - q_h\|_Q \|\mathbf{v}_h\|_1. \tag{4.28}$$

Then, using (4.27) and (4.28) in (4.23), we infer

$$\|p_h - q_h\|_Q \leq Ch^k \left(|\mathbf{f}|_{k-1} + |\mathbf{u}|_{k+1} \right) + C \|p - q_h\|_Q. \tag{4.29}$$

Finally, using (4.29) and the triangular inequality, we get

$$\|p - p_h\|_Q \leq \|p - q_h\|_Q + \|p_h - q_h\|_Q \leq Ch^k \left(|\mathbf{f}|_{k-1} + |\mathbf{u}|_{k+1} \right) + C \|p - q_h\|_Q \qquad \forall\, q_h \in Q_h.$$

Passing to the infimum with respect to $q_h \in Q_h$, and using estimate (4.19), we obtain (4.22). □

5. Reduced spaces and reduced problem

In this section we show that problem (3.32) is equivalent to a suitable reduced problem (*cf.* Prop. 5.1), involving significantly fewer degrees of freedom, especially for large k. Let us define the reduced local virtual spaces, for $k \geq 2$:

$$\widehat{\mathbf{V}}_h^K \quad := \quad \left\{ \mathbf{v} \in [H^1(K)]^2 \quad \text{s.t} \quad \mathbf{v}_{|\partial K} \in [\mathbb{B}_k(\partial K)]^2, \begin{cases} -\,\nu\, \boldsymbol{\Delta} \mathbf{v} - \nabla s \in \mathcal{G}_{k-2}(K)^{\perp}, \\ \operatorname{div} \mathbf{v} \in \mathbb{P}_0(K), \end{cases} \quad \text{for some } s \in H^1(K) \right\} \tag{5.1}$$

and

$$\widehat{Q}_h^K := \mathbb{P}_0(K). \tag{5.2}$$

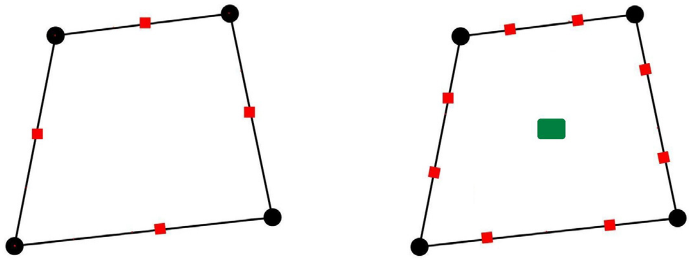

FIGURE 2. Degrees of freedom for $k = 2$, $k = 3$. We denote $\widehat{\mathbf{D}}_{\mathbf{V}}\mathbf{1}$ with the black dots, $\widehat{\mathbf{D}}_{\mathbf{V}}\mathbf{2}$ with the red squares, $\widehat{\mathbf{D}}_{\mathbf{V}}\mathbf{3}$ with the green rectangles. (Color online)

Moreover, we have:

$$\dim\left(\widehat{\mathbf{V}}_h^K\right) = \dim\left([\mathbb{B}_k(\partial K)]^2\right) + \dim\left(\mathcal{G}_{k-2}(K)^\perp\right) = 2n_K k + \frac{(k-1)(k-2)}{2}, \tag{5.3}$$

and

$$\dim(\widehat{Q}_h^K) = \dim(\mathbb{P}_0(K)) = 1, \tag{5.4}$$

where n_K is the number of edges in ∂K. As sets of degrees of freedom for the reduced spaces, we may consider the following.

For every function $\mathbf{v} \in \widehat{\mathbf{V}}_h^K$ we take the following linear operators $\widehat{\mathbf{D}}_{\mathbf{V}}$, split into three subsets (see Fig. 2):

- $\widehat{\mathbf{D}}_{\mathbf{V}}\mathbf{1}$: the values of $\mathbf{v}$ at each vertex of the polygon K,
- $\widehat{\mathbf{D}}_{\mathbf{V}}\mathbf{2}$: the values of $\mathbf{v}$ at $k-1$ distinct points of every edge $e \in \partial K$,
- $\widehat{\mathbf{D}}_{\mathbf{V}}\mathbf{3}$: the moments of $\mathbf{v}$

$$\int_K \mathbf{v} \cdot \mathbf{g}_{k-2}^\perp \, \mathrm{d}K \qquad \text{for all } \mathbf{g}_{k-2}^\perp \in \mathcal{G}_{k-2}(K)^\perp.$$

For every $q \in \widehat{Q}_h$ we consider

- $\widehat{\mathbf{D}}_{\mathbf{Q}}$: the moment

$$\int_K q \, \mathrm{d}K.$$

We define the global reduced virtual element spaces by setting

$$\widehat{\mathbf{V}}_h := \{\mathbf{v} \in [H_0^1(\Omega)]^2 \quad \text{s.t} \quad \mathbf{v}_{|K} \in \widehat{\mathbf{V}}_h^K \quad \text{for all } K \in \mathcal{T}_h\} \tag{5.5}$$

and

$$\widehat{Q}_h := \{q \in L_0^2(\Omega) \quad \text{s.t.} \quad q_{|K} \in \widehat{Q}_h^K \quad \text{for all } K \in \mathcal{T}_h\}. \tag{5.6}$$

It is easy to check that

$$\dim(\widehat{\mathbf{V}}_h) = n_P \frac{(k-1)(k-2)}{2} + 2(n_V + (k-1)n_E) \tag{5.7}$$

and

$$\dim(\widehat{Q}_h) = n_P - 1 \tag{5.8}$$

where we recall that n_P is the number of elements in $\mathcal{T}_h$, n_E and n_V are respectively the number of internal edges and internal vertexes in the decomposition.

The reduced virtual element discretization of the Stokes problem (2.6) is then:

$$\begin{cases} \text{find } \widehat{\mathbf{u}}_h \in \widehat{\mathbf{V}}_h \text{ and } \widehat{p}_h \in \widehat{Q}_h, \text{ such that} \\ a_h(\widehat{\mathbf{u}}_h, \widehat{\mathbf{v}}_h) + b(\widehat{\mathbf{v}}_h, \widehat{p}_h) = (\mathbf{f}_h, \widehat{\mathbf{v}}_h) & \text{for all } \widehat{\mathbf{v}}_h \in \widehat{\mathbf{V}}_h, \\ b(\widehat{\mathbf{u}}_h, \widehat{q}_h) = 0 & \text{for all } \widehat{q}_h \in \widehat{Q}_h. \end{cases} \tag{5.9}$$

Above, the bilinear forms $a_h(\cdot,\cdot)$ and $b(\cdot,\cdot)$, and the loading term $\mathbf{f}_h$ are the same as before, see (3.29), (3.19) and (3.30). It is easily seen that all the terms involved in (5.9) are computable by means of the new reduced degrees of freedom. For example, to compute $(\mathbf{f}_h, \widehat{\mathbf{v}}_h)$ one needs to compute $\Pi^{0,K}_{k-2}\widehat{\mathbf{v}}_h$, see (3.31). However, for any $\mathbf{q}_{k-2} \in [\mathbb{P}_{k-2}(K)]^2$ we have:

$$\int_K \Pi^{0,K}_{k-2}\widehat{\mathbf{v}}_h \cdot \mathbf{q}_{k-2}\,\mathrm{d}K = \int_K \widehat{\mathbf{v}}_h \cdot \mathbf{q}_{k-2}\,\mathrm{d}K = \int_K \widehat{\mathbf{v}}_h \cdot \nabla q_{k-1}\,\mathrm{d}K + \int_K \widehat{\mathbf{v}}_h \cdot \mathbf{g}^{\perp}_{k-2}\,\mathrm{d}K$$

for suitable $q_{k-1} \in \mathbb{P}_{k-1}(K)$ and $\mathbf{g}^{\perp}_{k-2} \in \mathcal{G}_{k-2}(K)^{\perp}$. Then, since $\operatorname{div}\widehat{\mathbf{v}}_h \in \mathbb{P}_0(K)$, denoting with $|K|$ the area of K, we get

$$\begin{aligned} \int_K \Pi^{0,K}_{k-2}\widehat{\mathbf{v}}_h \cdot \mathbf{q}_{k-2}\,\mathrm{d}K &= -\int_K \operatorname{div}\widehat{\mathbf{v}}_h\, q_{k-1}\,\mathrm{d}K + \int_{\partial K} q_{k-1}\widehat{\mathbf{v}}_h \cdot \mathbf{n}\,\mathrm{d}s + \int_K \widehat{\mathbf{v}}_h \cdot \mathbf{g}^{\perp}_{k-2}\,\mathrm{d}K \\ &= -|K|^{-1}\left(\int_{\partial K} \widehat{\mathbf{v}}_h \cdot \mathbf{n}\,\mathrm{d}s\right)\int_K q_{k-1}\,\mathrm{d}K + \int_{\partial K} q_{k-1}\widehat{\mathbf{v}}_h \cdot \mathbf{n}\,\mathrm{d}s + \int_K \widehat{\mathbf{v}}_h \cdot \mathbf{g}^{\perp}_{k-2}\,\mathrm{d}K \end{aligned}$$

whose right-hand side is directly computable from $\widehat{\mathbf{D}}_{\mathbf{V}}$.

In addition, using the same techniques of Proposition 4.3 (take $\pi_h\mathbf{v} = \bar{\mathbf{v}}_h$ in the proof), one can prove that

$$\exists\, \widehat{\beta} > 0 \quad \text{such that} \quad \sup_{\widehat{\mathbf{v}}_h \in \widehat{\mathbf{V}}_h\, \widehat{\mathbf{v}}_h \neq \mathbf{0}} \frac{b(\widehat{\mathbf{v}}_h, \widehat{q}_h)}{\|\widehat{\mathbf{v}}_h\|_1} \geq \widehat{\beta}\|\widehat{q}_h\|_Q \qquad \text{for all } \widehat{q}_h \in \widehat{Q}_h. \tag{5.10}$$

The following proposition states the relation between problem (3.32) and the reduced problem (5.9).

Proposition 5.1. *Let $(\mathbf{u}_h, p_h) \in \mathbf{V}_h \times Q_h$ be the solution of problem (3.32) and $(\widehat{\mathbf{u}}_h, \widehat{p}_h) \in \widehat{\mathbf{V}}_h \times \widehat{Q}_h$ be the solution of problem (5.9). Then*

$$\widehat{\mathbf{u}}_h = \mathbf{u}_h \qquad \text{and} \qquad \widehat{p}_{h|K} = \Pi^{0,K}_0 p_h \quad \text{for all } K \in \mathcal{T}_h. \tag{5.11}$$

Proof. Let

$$\widehat{\mathbf{Z}}_h := \{\widehat{\mathbf{v}}_h \in \widehat{\mathbf{V}}_h \quad \text{s.t.} \quad b(\widehat{\mathbf{v}}_h, \widehat{q}_h) = 0 \quad \text{for all } \widehat{q}_h \in \widehat{Q}_h\}.$$

Then $\widehat{\mathbf{u}}_h$ solves (*cf.* (4.21)):

$$\begin{cases} \text{find } \widehat{\mathbf{u}}_h \in \widehat{\mathbf{Z}}_h \\ a_h(\widehat{\mathbf{u}}_h, \widehat{\mathbf{v}}_h) = (\mathbf{f}_h, \widehat{\mathbf{v}}_h) & \text{for all } \widehat{\mathbf{v}}_h \in \widehat{\mathbf{Z}}_h. \end{cases} \tag{5.12}$$

We now notice that $\widehat{\mathbf{Z}}_h = \mathbf{Z}_h$, see (3.34). Therefore, problem (5.12) is equivalent to problem (4.21) and $\widehat{\mathbf{u}}_h = \mathbf{u}_h$.

For the pressure component of the solution, from (3.32) and (5.9), we get

$$b(\mathbf{v}_h, p_h) = (\mathbf{f}_h, \mathbf{v}_h) - a_h(\mathbf{u}_h, \mathbf{v}_h) \qquad \text{for all } \mathbf{v}_h \in \mathbf{V}_h \tag{5.13}$$

$$b(\widehat{\mathbf{v}}_h, \widehat{p}_h) = (\mathbf{f}_h, \widehat{\mathbf{v}}_h) - a_h(\widehat{\mathbf{u}}_h, \widehat{\mathbf{v}}_h) \qquad \text{for all } \widehat{\mathbf{v}}_h \in \widehat{\mathbf{V}}_h. \tag{5.14}$$

TABLE 1. Percentage saving of DoFs in the reduced problem with respect the original one.

		$k=2$	$k=3$	$k=4$	$k=5$
$\mathcal{V}_h$	$h=1/4$	34.408%	43.715%	48.484%	51.494%
	$h=1/8$	30.260%	39.506%	44.547%	47.863%
	$h=1/16$	28.460%	37.624%	42.753%	46.185%
	$h=1/32$	27.634%	36.749%	41.911%	45.392%
$\mathcal{T}_h$	$h=1/2$	49.230%	56.737%	59.751%	61.369%
	$h=1/4$	47.761%	55.427%	58.616%	60.377%
	$h=1/8$	45.937%	53.889%	57.314%	59.253%
	$h=1/16$	45.171%	53.243%	56.767%	58.780%
$\mathcal{Q}_h$	$h=1/4$	43.835%	52.287%	56.031%	58.181%
	$h=1/8$	39.875%	48.706%	52.892%	55.411%
	$h=1/16$	38.066%	47.041%	51.417%	54.098%
	$h=1/32$	37.202%	46.238%	50.701%	53.458%

Let $p_h =: p_0 + p^\perp$, where $p_{0|K} = \Pi_0^{0,K} p_h$ for all $K \in \mathcal{T}_h$, and $p^\perp := p_h - p_0$ (hence $\int_K p^\perp \,\mathrm{d}K = 0$). From (5.13), we have

$$b(\mathbf{v}_h, p_0 + p^\perp) = (\mathbf{f}_h, \mathbf{v}_h) - a_h(\mathbf{u}_h, \mathbf{v}_h) \qquad \text{for all } \mathbf{v}_h \in \mathbf{V}_h.$$

Since $\widehat{\mathbf{V}}_h \subseteq \mathbf{V}_h$, we deduce

$$b(\widehat{\mathbf{v}}_h, p_0) + b(\widehat{\mathbf{v}}_h, p^\perp) = (\mathbf{f}_h, \widehat{\mathbf{v}}_h) - a_h(\mathbf{u}_h, \widehat{\mathbf{v}}_h) \qquad \text{for all } \widehat{\mathbf{v}}_h \in \widehat{\mathbf{V}}_h.$$

Now, $b(\widehat{\mathbf{v}}_h, p^\perp) = 0$ because $\operatorname{div} \widehat{\mathbf{v}}_h$ is constant on each polygon K. We conclude that

$$b(\widehat{\mathbf{v}}_h, p_0) = (\mathbf{f}_h, \widehat{\mathbf{v}}_h) - a_h(\mathbf{u}_h, \widehat{\mathbf{v}}_h) \qquad \text{for all } \widehat{\mathbf{v}}_h \in \widehat{\mathbf{V}}_h. \tag{5.15}$$

From (5.15) and recalling that $\mathbf{u}_h = \widehat{\mathbf{u}}_h$, we get that $(\widehat{\mathbf{u}}_h, p_0) \in \widehat{\mathbf{V}}_h \times \widehat{Q}_h$ solves problem (5.9). Uniqueness of the solution of problem (5.9) then implies $\widehat{p}_{h|K} = p_{0|K}$ for every K, and (5.11) is proved. □

Remark 5.2. Proposition 5.1 allows us to solve the Stokes problem (2.6) directly by making use of the reduced problem (5.9), saving $n_P((k+1)k-2)$ degrees of freedom, see (3.15), (3.16), (5.7) and (5.8). In Table 1 we display this quantity (with respect the total amount of the original DoFs) for the sequences of meshes introduced in Section 6 with $k = 2, 3, 4, 5$ in order to have an estimate of the saving in the reduced linear system with respect its original size.

In addition, we remark that Proposition 5.1 holds not only when homogeneous Dirichlet conditions are applied on the whole boundary, but also for other (possibly non-homogeneous) boundary conditions, as numerically shown in Section 6. We finally note that another method with high order precision but piecewise constant pressure can be found in [37].

Remark 5.3. It is possible to give an alternative proof of Proposition 5.1 directly in terms of the associated linear system (see [13]). Furthermore, it is also possible to implement the "reduced" problem (5.9) by coding the "complete" Stokes problem (3.32) and locally removing the rows and the columns relative to the extra degrees of freedom.

Remark 5.4. Given the solution of (5.9), if one is interested in a more accurate pressure, the discrete scalar field p_h can be recovered by an element-wise post-processing procedure. Such local problems can be, for instance, immediately extracted from the removed rows and columns mentioned in Remark 5.3.

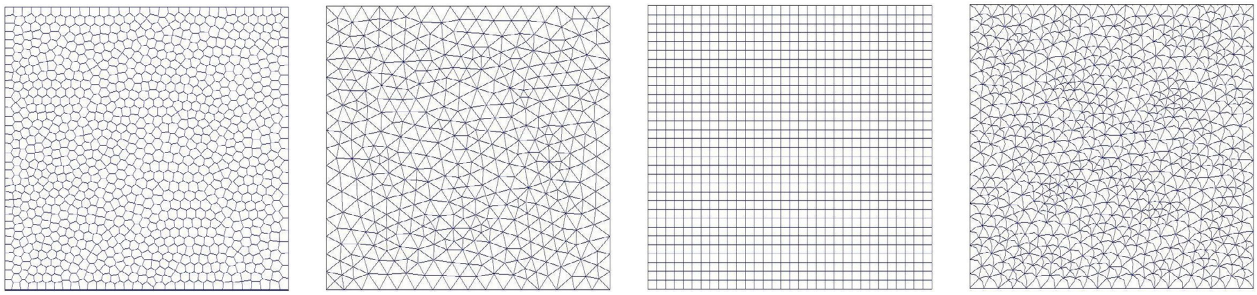

FIGURE 3. Example of polygonal meshes: $\mathcal{V}_{1/32}$, $\mathcal{T}_{1/16}$, $\mathcal{Q}_{1/32}$, $\mathcal{W}_{1/20}$.

6. Numerical tests

In this section we present two numerical experiments to test the actual performance of the method. In the first test we compare the reduced method introduced in Section 5 with the method presented in [8] (cf. Rem. 3.4). In the second experiment we investigate numerically the equivalence proved in Proposition 5.1, considering the more general case of non-homogeneous boundary conditions.

Before proceeding, we first recall that the VEM solution $\mathbf{u}_h$ is not explicitly known point-wise inside the elements. Therefore, the method error is not computable even when the analytical solution $\mathbf{u}$ is available. As usual in the VEM framework, we then compute the method error comparing $\mathbf{u}$ with a suitable polynomial projection of $\mathbf{u}_h$. To this end, for a given element $K \in \mathcal{T}_h$ and $k \geq 2$, we now introduce the tensor-valued L^2-projection operator $\boldsymbol{\Pi}^{0,K}_{k-1} \colon [L^2(K)]^{2\times 2} \to [\mathbb{P}_{k-1}(K)]^{2\times 2}$, defined by

$$\int_K \left(\mathbf{A} - \boldsymbol{\Pi}^{0,K}_{k-1}\mathbf{A}\right) : \mathbf{P}_{k-1}\,\mathrm{d}x = 0 \qquad \text{for all } \mathbf{A} \in [L^2(\Omega)]^{2\times 2} \text{ and } \mathbf{P}_{k-1} \in [\mathbb{P}_{k-1}(K)]^{2\times 2}. \tag{6.1}$$

Following a similar argument as in Section 3.2, it is easy to derive that for every $\mathbf{v}_h$ in $\mathbf{V}_h$ (resp. in $\widehat{\mathbf{V}}_h$), $\boldsymbol{\Pi}^{0,K}_{k-1}\,\boldsymbol{\nabla}\mathbf{v}_h$ is exactly computable using the DoFs $\mathbf{D}_{\mathbf{V}}$ (resp. $\widehat{\mathbf{D}}_{\mathbf{V}}$). Similar arguments allow to compute $\boldsymbol{\Pi}^{0,K}_{k-1}\,\boldsymbol{\nabla}\mathbf{v}_h$ for all $\mathbf{v}_h$ in the virtual space $\widetilde{\mathbf{V}}_h$ using the DoFs $\widetilde{\mathbf{D}}_{\mathbf{V}}$ (see Rem. 3.4).

Regarding the computational domain, in our tests we always take the square domain $\Omega = [0,1]^2$, which is partitioned using the following sequences of polygonal meshes:

- $\{\mathcal{V}_h\}_h$: sequence of Voronoi meshes with $h = 1/4, 1/8, 1/16, 1/32$,
- $\{\mathcal{T}_h\}_h$: sequence of triangular meshes with $h = 1/2, 1/4, 1/8, 1/16$,
- $\{\mathcal{Q}_h\}_h$: sequence of square meshes with $h = 1/4, 1/8, 1/16, 1/32$.
- $\{\mathcal{W}_b\}_h$: sequence of WEB-like meshes with $h = 4/10, 2/10, 1/10, 1/20$.

An example of the adopted meshes is shown in Figure 3. For the generation of the Voronoi meshes we used the code Polymesher [48]. The WEB-like meshes are composed by hexagons, generated starting from the triangular meshes $\{\mathcal{T}_h\}_h$ and randomly displacing the midpoint of each (non boundary) edge. In the tests we set $\nu = 1$.

Test 6.1. In this example, we apply homogeneous boundary conditions on the whole $\partial\Omega$, and we choose the load term $\mathbf{f}$ in such a way that the analytical solution is

$$\mathbf{u}(x,y) = \begin{pmatrix} -\frac{1}{2}\,\cos^2(x)\cos(y)\sin(y) \\ \frac{1}{2}\,\cos^2(y)\cos(x)\sin(x) \end{pmatrix} \qquad p(x,y) = \sin(x) - \sin(y).$$

We make use of the projection operator in (6.1) and consider the error quantities:

$$\delta(\mathbf{u}) := \left(\sum_{K\in\mathcal{T}_h} \left\|\boldsymbol{\nabla}\, u - \boldsymbol{\Pi}^{0,K}_{k-1}(\boldsymbol{\nabla}\, u_h)\right\|^2_{0,K}\right)^{1/2} \qquad \text{and} \qquad \delta(p) := \|p - p_h\|_0. \tag{6.2}$$

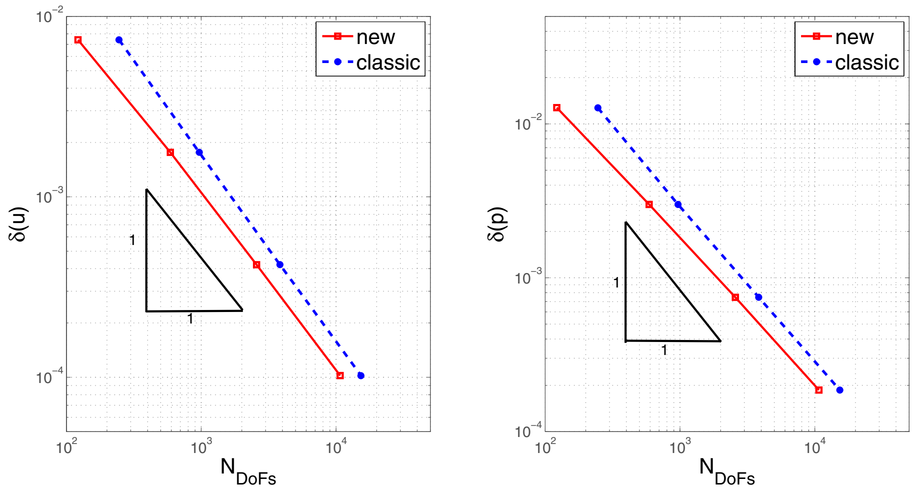

FIGURE 4. Test 6.1: Behaviour of $\delta(\mathbf{u})$ and $\delta(p)$ for the sequence of meshes $\mathcal{V}_h$ with $k = 2$.

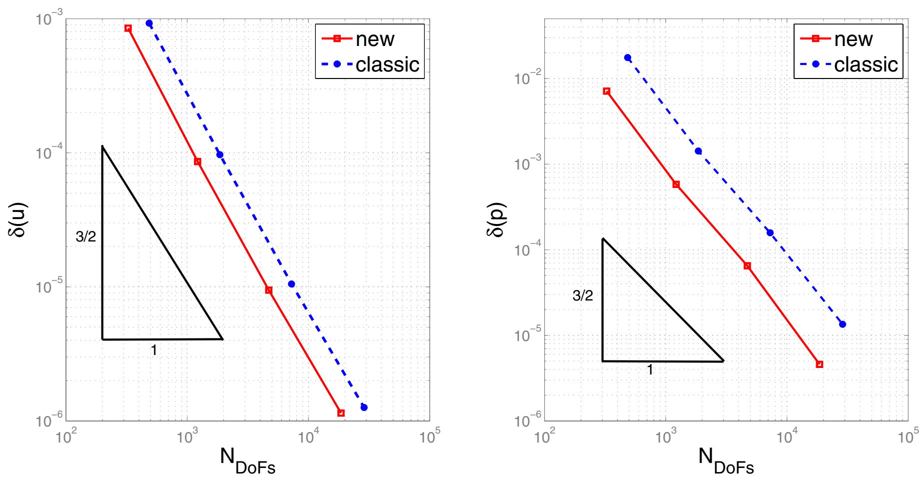

FIGURE 5. Test 6.1: Behaviour of $\delta(\mathbf{u})$ and $\delta(p)$ for the sequence of meshes $\mathcal{V}_h$ with $k = 3$.

We compare two different methods, by studying $\delta(\mathbf{u})$ and $\delta(p)$ versus the total number of degrees of freedom N_{DoFs}. The first method is the reduced scheme of Section 5 (labeled as "new"), with the post-processed pressure of Remark 5.4. The second method is the scheme of [8] extended to the Stokes problem (see Rems. 3.4 and 4.5), labeled as "classic". In both cases we consider polynomial degrees $k = 2, 3$.

In Figures 4 and 5, we display the results for the sequence of Voronoi meshes $\mathcal{V}_h$. In Figures 6 and 7, we show the results for the sequence of meshes $\mathcal{T}_h$, while in Figures 8 and 9 we plot the results for the sequence of meshes $\mathcal{Q}_h$, finally in Figures 10 and 11 we exhibit the results for the sequence of meshes $\mathcal{W}_h$.

We notice that the theoretical predictions of Sections 4 and 5 are confirmed (noticed that the method error and N_{dof} behave like h^k and h^{-2}, respectively). Moreover, we observe that the reduced method exhibit significant smaller errors than the standard method, at least for this example and with the adopted meshes.

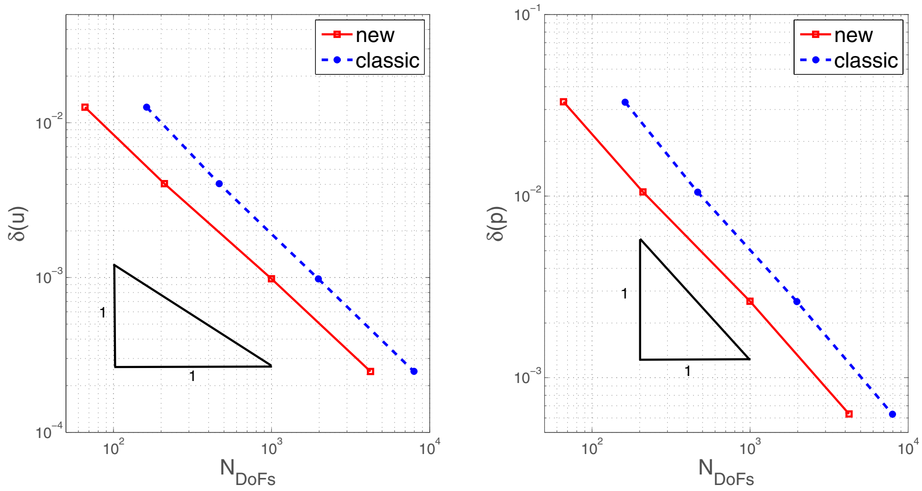

FIGURE 6. Test 6.1: Behaviour of $\delta(\mathbf{u})$ and $\delta(p)$ for the sequence of meshes $\mathcal{T}_h$ with $k = 2$.

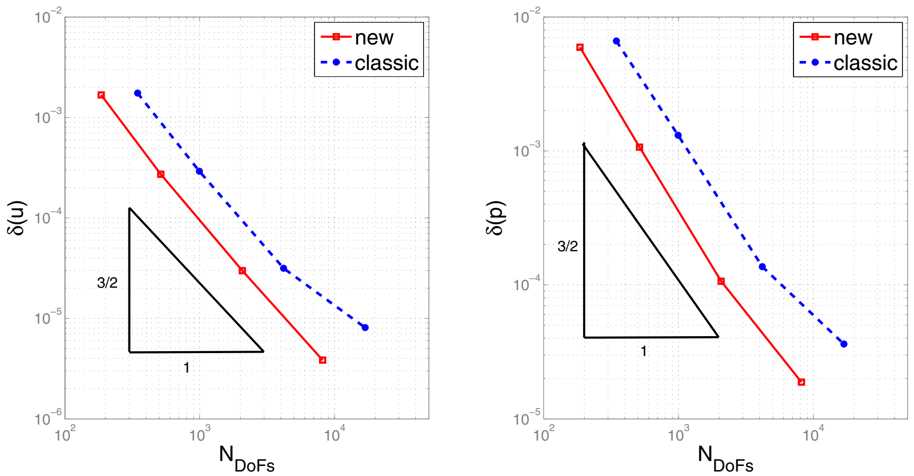

FIGURE 7. Test 6.1: Behaviour of $\delta(\mathbf{u})$ and $\delta(p)$ for the sequence of meshes $\mathcal{T}_h$ with $k = 3$.

Test 6.2. In this example we choose the load term $\mathbf{f}$ and the *non-homogeneous* polynomial Dirichlet boundary conditions in such a way that the analytical solution is

$$\mathbf{u}(x, y) = \begin{pmatrix} y^4 + 1 \\ x^4 + 2 \end{pmatrix} \qquad p(x, y) = x^3 - y^3.$$

The aim of this test is to check numerically the results of Proposition 5.1; in order to be more general, we consider the case of non-homogeneous boundary conditions. Let $(\mathbf{u}_h, p_h)$ be the solution of problem (3.32) and $(\widehat{\mathbf{u}}_h, \widehat{p}_h)$ be the solution of problem (5.9). As a measure of discrepancy between the two solutions, we introduce the error quantities

$$\varepsilon(\mathbf{u}) := \left(\sum_{K \in \mathcal{T}_h} \left\| \boldsymbol{\Pi}^{0,K}_{k-1} \boldsymbol{\nabla}(\mathbf{u}_h - \widehat{\mathbf{u}}_h) \right\|^2_{0,K} \right)^{1/2} \qquad \varepsilon(p) := \left(\sum_{K \in \mathcal{T}_h} \left\| \Pi^{0,K}_0 p_h - \widehat{p}_h \right\|^2_{0,K} \right)^{1/2}.$$

In Table 2 we display the values of $\varepsilon(\mathbf{u})$ and $\varepsilon(p)$ for the family of meshes $\mathcal{V}_h$, $\mathcal{T}_h$ and $\mathcal{Q}_h$, choosing $k = 2, 3$.

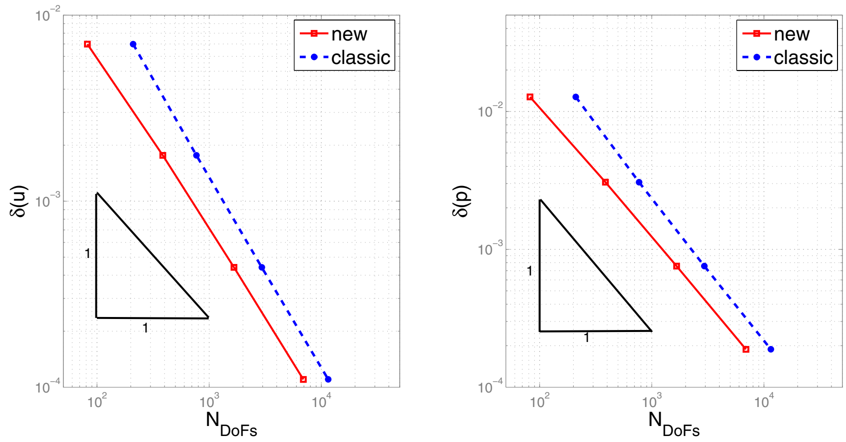

FIGURE 8. Test 6.1: Behaviour of $\delta(\mathbf{u})$ and $\delta(p)$ for the sequence of meshes $\mathcal{Q}_h$ with $k = 2$.

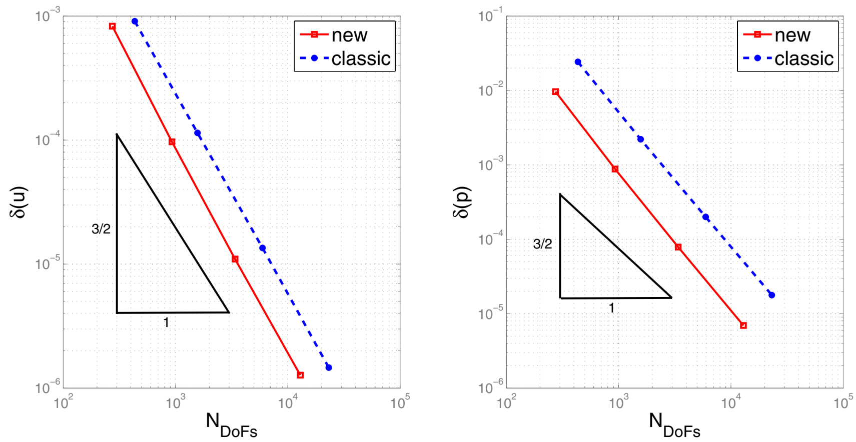

FIGURE 9. Test 6.1: Behaviour of $\delta(\mathbf{u})$ and $\delta(p)$ for the sequence of meshes $\mathcal{Q}_h$ with $k = 3$.

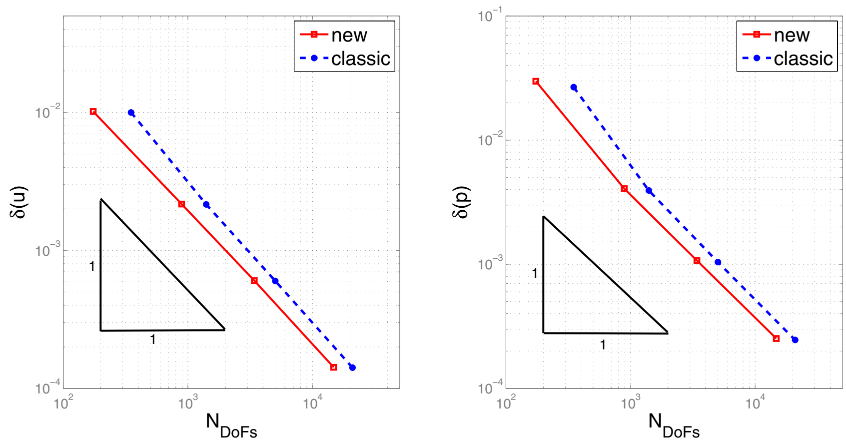

FIGURE 10. Test 6.1: Behaviour of $\delta(\mathbf{u})$ and $\delta(p)$ for the sequence of meshes $\mathcal{W}_h$ with $k = 2$.

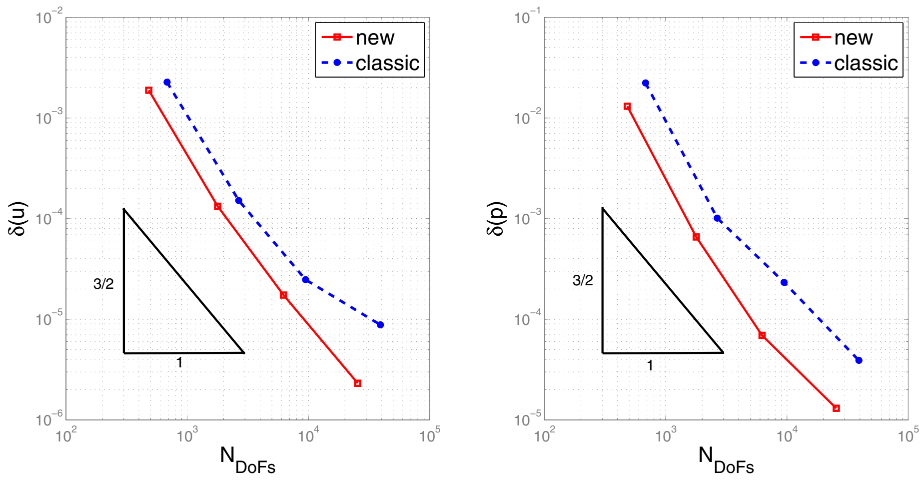

FIGURE 11. Test 6.1: Behaviour of $\delta(\mathbf{u})$ and $\delta(p)$ for the sequence of meshes $\mathcal{W}_h$ with $k = 3$.

TABLE 2. Test 6.2: $\varepsilon(\mathbf{u})$ and $\varepsilon(p)$ for the meshes $\mathcal{V}_h$, $\mathcal{T}_h$, $\mathcal{Q}_h$, $\mathcal{W}_h$ with $k = 2, 3$.

		$k=2$		$k=3$	
		$\varepsilon(\mathbf{u})$	$\varepsilon(p)$	$\varepsilon(\mathbf{u})$	$\varepsilon(p)$
$\mathcal{V}_h$	$h = 1/4$	1.8366063e−13	1.2397027e−13	9.9584405e−12	9.5750683e−13
	$h = 1/8$	5.6291757e−13	1.7037760e−13	1.0257081e−11	6.4888535e−13
	$h = 1/16$	1.5395183e−12	5.3823612e−13	1.2017070e−11	1.5761308e−12
	$h = 1/32$	3.5162644e−12	5.2896229e−13	2.7289064e−11	9.7059278e−12
$\mathcal{T}_h$	$h = 1/2$	1.6148091e−13	2.7158830e−14	5.3139688e−12	9.5716694e−13
	$h = 1/4$	4.1349069e−13	6.9691214e−14	9.1204063e−11	4.8537564e−13
	$h = 1/8$	1.3353440e−12	1.0109968e−13	2.7989324e−11	8.0028046e−12
	$h = 1/16$	3.1038037e−12	2.3636051e−13	2.4258164e−11	1.4188633e−11
$\mathcal{Q}_h$	$h = 1/4$	1.6747387e−13	8.0270859e−14	8.0510701e−12	2.1761282e−13
	$h = 1/8$	4.3127288e−13	1.7217954e−13	2.9673107e−12	1.5735525e−13
	$h = 1/16$	1.0294053e−12	2.2290502e−13	4.2024937e−12	7.9220732e−13
	$h = 1/32$	2.4711285e−12	2.4074145e−13	7.6167571e−12	5.9492426e−13
$\mathcal{W}_h$	$h = 4/10$	9.1587957e−13	7.5286364e−14	1.6072996e−11	1.0673512e−13
	$h = 2/10$	1.3107628e−12	1.1154735e−13	1.2916868e−11	2.8184370e−13
	$h = 1/10$	4.0885427e−12	3.8760675e−13	5.2532025e−11	7.5670394e−13
	$h = 1/20$	7.2877771e−12	6.6196792e−13	8.4382876e−11	1.6915676e−12

Since the values of $\varepsilon(\mathbf{u})$ and $\varepsilon(p)$ are numerically negligible, we infer that the results of Proposition 5.1 are satisfied also in this case of *non-homogeneous* Dirichlet boundary conditions. Moreover we have also checked the maximum velocity error at all nodes of the mesh skeleton

$$\max_{\mathsf{v} \in \mathcal{V}_h} \|\mathbf{u}_h(\mathsf{v}) - \widehat{\mathbf{u}}_h(\mathsf{v})\|,$$

obtaining extremely small errors as well.

Appendix. The three-dimensional case

The aim of this section is to present a brief discussion about the extension of the proposed method to the three-dimensional case, taking advantage of the ideas developed for the two dimensional case combined with the construction in [1].

Let $\{\mathcal{T}_h\}_h$ be a sequence of decompositions of Ω into general polyhedral elements K. We assume that for all h, each element $K \in \mathcal{T}_h$ fulfills the following assumptions. There exists a positive constant γ such that:

- $(\mathbf{A1^{3D}})$ K is star-shaped with respect to a sphere of radius $\geq \gamma\, h_K$, and every face f of K is star-shaped with respect to a ball of radius $\geq \gamma\, h_f$,
- $(\mathbf{A2^{3D}})$ for every face f of K and for every edge e of f, it holds that

$$h_e \geq \gamma\, h_f \geq \gamma^2\, h_K,$$

where h_f (resp. h_e) denotes the diameter of the face f (resp. the length of the edge e).

Let K in $\mathcal{T}_h$. For every face $f \in \partial K$ we define the augmented virtual local-face space $\widetilde{\mathbf{W}}_h^f$

$$\widetilde{\mathbf{W}}_h^f = \left\{\mathbf{w} \in [H^1(f)]^3 \quad \text{s.t.} \quad \mathbf{w}_{|\partial f} \in [\mathbb{B}_k(\partial f)]^3,\ \boldsymbol{\Delta}\mathbf{w} \in [\mathbb{P}_k(f)]^3\right\}.$$

We now define the enhanced Virtual Element-face space $\mathbf{W}_h^f$ as

$$\mathbf{W}_h^f := \left\{\mathbf{w} \in \widetilde{\mathbf{W}}_h^f \quad \text{s.t.} \quad \left(\mathbf{w} - \Pi_k^{\nabla,f}\mathbf{w},\, \mathbf{q}\right)_{L^2(f)} = 0 \quad \text{for all } \mathbf{q} \in [\mathbb{P}_k(f)/\mathbb{P}_{k-2}(f)]^3\right\}. \tag{A.1}$$

Above, $\mathbb{P}_k(f)/\mathbb{P}_{k-2}(f)$ denotes the polynomials of degree $\leq k$ defined on f, that are $L^2(f)-$orthogonal to all the polynomials of degree $\leq k-2$. Furthermore, $\Pi_k^{\nabla,f}$ is the (face) energy projection operator analog to the one defined in (3.26). We also define the Virtual Element-boundary space $\mathbf{W}_h(\partial K)$ as

$$\mathbf{W}_h(\partial K) := \left\{\mathbf{w} \in [C^0(\partial K)]^3 \quad \text{s.t.} \quad \mathbf{w}_{|f} \in \mathbf{W}_h^f \quad \text{for all face } f \in \partial K\right\}. \tag{A.2}$$

The boundary space above is the vector-valued analog of the scalar-valued space introduced in [1] (more precisely, equation (26) of [1]). The present space is instead different inside the element, as shown below. We define the following finite dimensional local virtual spaces:

$$\mathbf{V}_h^K := \left\{\mathbf{v} \in [H^1(K)]^3 \quad \text{s.t} \quad \mathbf{v}_{|\partial K} \in \mathbf{W}_h(\partial K),\ \begin{cases} -\nu\,\boldsymbol{\Delta}\mathbf{v} - \nabla s \in \mathcal{G}_{k-2}(K)^{\perp}, \\ \operatorname{div}\mathbf{v} \in \mathbb{P}_{k-1}(K), \end{cases} \text{for some } s \in L^2(K)\right\}. \tag{A.3}$$

Above, $\mathcal{G}_{k-2}(K)^{\perp}$ is the 3D analog of the corresponding space introduced in Section 3.1. Given a function $\mathbf{v} \in \mathbf{V}_h^K$ we take the following linear operators $\mathbf{D_V}^{\mathbf{3D}}$, collected into five subsets:

- $\mathbf{D_V1^{3D}}$: the values of $\mathbf{v}$ at the vertices of the polygon K,
- $\mathbf{D_V2^{3D}}$: the values of $\mathbf{v}$ at $k-1$ distinct points of every edge e in K,
- $\mathbf{D_V3^{3D}}$: the moments up to order $k-2$ of $\mathbf{v}$ of every face f in K, *i.e.*

$$\int_f \mathbf{v}\cdot\mathbf{q}_{k-2}\,\mathrm{d}f \qquad \text{for all } \mathbf{q}_{k-2} \in [\mathbb{P}_{k-2}(f)]^3,$$

- $\mathbf{D_V4^{3D}}$: the moments of $\mathbf{v}$

$$\int_K \mathbf{v}\cdot\mathbf{g}_{k-2}^{\perp}\,\mathrm{d}K \qquad \text{for all } \mathbf{g}_{k-2}^{\perp} \in \mathcal{G}_{k-2}(K)^{\perp},$$

- $\mathbf{D_V5^{3D}}$: the moments up to order $k-1$ and greater than zero of $\operatorname{div}\mathbf{v}$ in K, *i.e.*

$$\int_K (\operatorname{div}\mathbf{v})\, q_{k-1}\, \mathrm{d}K \qquad \text{for all } q_{k-1} \in \mathbb{P}_{k-1}(K)/\mathbb{R}.$$

Combining the arguments in [1] and the results of Section 3 concerning the bi-dimensional case, it can be proved that:

- **(P1)**: the linear operators $\mathbf{D_V}$ $\mathbf{^{3D}}$ are a set of **degrees of freedom** for the space $\mathbf{V}_h^k$,
- **(P2)**: the linear operators $\mathbf{D_V1^{3D}}$, $\mathbf{D_V2^{3D}}$, $\mathbf{D_V3^{3D}}$ allow to compute

$$\int_f \mathbf{v}\cdot\mathbf{q}_k\, \mathrm{d}f$$

  for all $\mathbf{q}_k \in [\mathbb{P}_k(f)]^3$, for all $\mathbf{v} \in \mathbf{V}_h^K$, and for all face $f \in \partial K$.

For the pressure field, we take the three-dimensional analog to the space and DoFs of the bi-dimensional case (polynomials of degree $k-1$ inside the element).

Once the above spaces have been selected, the method design in the 3D setting follows the lines of Sections 3.2–3.4 verbatim. The *divergence-free property* of the discrete solution and, more generally, property (3.35), still hold true.

As far as the inf-sup condition is concerned, the same arguments in the proof of Proposition 4.3 can be applied for the three-dimensional case, as well. Indeed, recalling that $k \geq 2$, we observe that the 3D velocity approximation space has enough degrees of freedom on each face and in the interior of the polyhedra, to perform the construction of the operator π_h introduced in Proposition 4.3. It is beyond the scope of the present paper to show the details of such construction.

Acknowledgements. Giuseppe Vacca thanks the National Group of Scientific Computing (GNCS-INDAM) that supported this research through the project: "Finanziamento Giovani Ricercatori 2014-2015".

References

[1] B. Ahmad, A. Alsaedi, F. Brezzi, L.D. Marini and A. Russo, Equivalent projectors for virtual element methods. *Comput. Math. Appl.* **66** (2013) 376–391.

[2] P.F. Antonietti, S. Giani and P. Houston, *hp*-version composite discontinuous Galerkin methods for elliptic problems on complicated domains. *SIAM J. Sci. Comput.* **35** (2013) A1417–A1439.

[3] P.F. Antonietti, L. Beirão da Veiga, D. Mora and M. Verani, A stream virtual element formulation of the Stokes problem on polygonal meshes. *SIAM J. Numer. Anal.* **52** (2014) 386–404.

[4] L. Beirão da Veiga and G. Manzini, A virtual element method with arbitrary regularity. *IMA J. Numer. Anal.* **34** (2014) 759–781.

[5] L. Beirão da Veiga, V. Gyrya, K. Lipnikov and G. Manzini, Mimetic finite difference method for the Stokes problem on polygonal meshes. *J. Comput. Phys.* **228** (2009) 7215–7232.

[6] L. Beirão da Veiga, K. Lipnikov and G. Manzini, Arbitrary-order nodal mimetic discretizations of elliptic problems on polygonal meshes. *SIAM J. Numer. Anal.* **49** (2011) 1737–1760.

[7] L. Beirão da Veiga, F. Brezzi, A. Cangiani, G. Manzini, L. D. Marini and A. Russo, Basic principles of virtual element methods. *Math. Models Methods Appl. Sci.* **23** (2013) 199–214.

[8] L. Beirão da Veiga, F. Brezzi and L.D. Marini, Virtual elements for linear elasticity problems. *SIAM J. Numer. Anal.* **51** (2013) 794–812.

[9] L. Beirão da Veiga, F. Brezzi, L.D. Marini and A. Russo, The Hitchhiker's Guide to the Virtual Element Method. *Math. Models Methods Appl. Sci.* **24** (2014) 1541–1573.

[10] L. Beirão da Veiga, K. Lipnikov and G. Manzini, The mimetic finite difference method for elliptic problems. Vol. 11 of *MS&A. Modeling, Simulation and Applications.* Springer (2014).

[11] L. Beirão Da Veiga, F. Brezzi, L.D. Marini and A. Russo, $H(div)$ and $H(curl)$-conforming VEM. *Numer. Math.* (2015) 1–30.

[12] L. Beirão da Veiga, C. Lovadina and D. Mora, A virtual element method for elastic and inelastic problems on polytope meshes. *Comput. Methods Appl. Mech. Engrg.* **295** (2015) 327–346.

[13] L. Beirão Da Veiga, C. Lovadina and G. Vacca, Divergence free virtual elements for the Stokes problem on polygonal meshes. Preprint arXiv:1510.01655 (2015).

[14] M.F. Benedetto, S. Berrone, S. Pieraccini and S. Scialò, The virtual element method for discrete fracture network simulations. *Comput. Methods Appl. Mech. Engrg.* **280** (2014) 135–156.
[15] J.E. Bishop, A displacement-based finite element formulation for general polyhedra using harmonic shape functions. *Int. J. Numer. Methods Engrg.* **97** (2014) 1–31.
[16] D. Boffi, F. Brezzi and M. Fortin, Mixed finite element methods and applications. Vol. 44 of *Springer Series in Computational Mathematics*. Springer, Heidelberg (2013).
[17] J. Bonelle and A. Ern, Analysis of compatible discrete operator schemes for elliptic problems on polyhedral meshes. *ESAIM: M2AN* **48** (2014) 553–581.
[18] S.C. Brenner and L.R. Scott, The mathematical theory of finite element methods. Vol. 15 of *Texts in Applied Mathematics*, 3rd edition. Springer, New York (2008).
[19] F. Brezzi and L.D. Marini, Virtual element methods for plate bending problems. *Comput. Methods Appl. Mech. Engrg.* **253** (2013) 455–462.
[20] F. Brezzi, K. Lipnikov and M. Shashkov, Convergence of the mimetic finite difference method for diffusion problems on polyhedral meshes. *SIAM J. Numer. Anal.* **43** (2005) 1872–1896.
[21] F. Brezzi, A. Buffa and K. Lipnikov, Mimetic finite differences for elliptic problems. *ESAIM: M2AN* **43** (2009) 277–295.
[22] F. Brezzi, R. S. Falk and L.D. Marini, Basic principles of mixed virtual element methods. *ESAIM: M2AN* **48** (2014) 1227–1240.
[23] A. Buffa, C. de Falco and G. Sangalli, Isogeometric analysis: Stable elements for the 2d stokes equation. *Int. J. Numer. Methods Fluids* **65** (2011) 1407–1422.
[24] A. Cangiani, E.H. Georgoulis and P. Houston, hp-version discontinuous galerkin methods on polygonal and polyhedral meshes. *Math. Mod. Meth. Appl. Sci.* **24** (2014) 2009–2041.
[25] J. Carrero, B. Cockburn and D. Schötzau, Hybridized globally divergence-free LDG methods. I. The Stokes problem. *Math. Comp.* **75** (2006) 533–563.
[26] P. Clément, Approximation by finite element functions using local regularization. *RAIRO Anal. Numér.* **9** (1975) 77–84.
[27] B. Cockburn, G. Kanschat, D. Schötzau and C. Schwab, Local discontinuous Galerkin methods for the Stokes system. *SIAM J. Numer. Anal.* **40** (2002) 319–343.
[28] B. Cockburn, D. Schötzau and J. Wang, Discontinuous Galerkin methods for incompressible elastic materials. *Comput. Methods Appl. Mech. Engrg.* **195** (2006) 3184–3204.
[29] B. Cockburn, G. Kanschat and D. Schötzau, An equal-order DG method for the incompressible Navier–Stokes equations. *J. Sci. Comput.* **40** (2009) 188–210.
[30] M. Costabel and M. Dauge, On the Inequalities of Babuška–Aziz, Friedrichs and Horgan–Payne. *Arch. Ration. Mech. Anal.* **217** (2015) 873–898.
[31] D. Di Pietro and A. Ern, A hybrid high-order locking-free method for linear elasticity on general meshes. *Comput. Methods Appl. Mech. Engrg.* **283** (2015) 1–21.
[32] R.G. Durán, An elementary proof of the continuity from $L^2_0(\Omega)$ to $H^1_0(\Omega)^n$ of Bogovskii's right inverse of the divergence. *Rev. Un. Mat. Argentina* **53** (2012) 59–78.
[33] M. Fortin and F. Brezzi, *Mixed and hybrid finite element methods*. Springer-Verlag, New York (1991).
[34] A.L. Gain, C. Talischi and G.H. Paulino, On the virtual element method for three-dimensional linear elasticity problems on arbitrary polyhedral meshes. *Comput. Methods Appl. Mech. Engrg.* **282** (2014) 132–160.
[35] J. Guzmán and M. Neilan, Conforming and divergence-free Stokes elements in three dimensions. *IMA J. Numer. Anal.* **34** (2014) 1489–1508.
[36] J. Guzmán and M. Neilan, Conforming and divergence-free Stokes elements on general triangular meshes. *Math. Comp.* **83** (2014) 15–36.
[37] Y. Jeon, E.-J. Park and D. Sheen, A hybridized finite element method for the Stokes problem. *Comput. Math. Appl.* **68** (2014) 2222–2232.
[38] K. Lipnikov, D. Vassilev and I. Yotov, Discontinuous galerkin and mimetic finite difference methods for coupled stokes–darcy flows on polygonal and polyhedral grids. *Numer. Math.* **126** (2013) 321–360.
[39] K. Lipnikov, G. Manzini and M. Shashkov, Mimetic finite difference method. *J. Comput. Phys.* **257** (2014) 1163–1227.
[40] D. Mora, G. Rivera and R. Rodríguez, A virtual element method for the steklov eigenvalue problem. *Math. Models Methods Appl. Sci.* **25** (2015) 1421–1445.
[41] S.E. Mousavi and N. Sukumar, Numerical integration of polynomials and discontinuous functions on irregular convex polygons and polyhedrons. *Comput. Mech.* **47** (2011) 535–554.
[42] S. Natarajan, S. Bordas and D.R. Mahapatra, Numerical integration over arbitrary polygonal domains based on Schwarz–Christoffel conformal mapping. *Int. J. Numer. Meth. Eng.* **80** (2009) 103–134.
[43] A. Rand, A. Gillette and C. Bajaj, Interpolation error estimates for mean value coordinates over convex polygons. *Adv. Comput. Math.* **39** (2013) 327–347.
[44] S. Rjasanow and S. Weißer, Higher order bem-based fem on polygonal meshes. *SIAM J. Numer. Anal.* **50** (2012) 2357–2378.
[45] N. Sukumar and A. Tabarraei, Conforming polygonal finite elements. *Int. J. Numer. Meth. Eng.* **61** (2004) 2045–2066.
[46] C. Talischi and G.H. Paulino, Addressing integration error for polygonal finite elements through polynomial projections: a patch test connection. *Math. Models Methods Appl. Sci.* **24** (2014) 1701–1727.
[47] C. Talischi, G.H. Paulino, A. Pereira and I.F.M. Menezes, Polygonal finite elements for topology optimization: a unifying paradigm. *Int. J. Numer. Meth. Eng.* **82** (2010) 671–698.

[48] C. Talischi, G.H. Paulino, A. Pereira and I.F.M. Menezes, Polymesher: a general-purpose mesh generator for polygonal elements written in matlab. *Struct. Multidisc Optimiz.* **45** (2012) 309–328.

[49] G. Vacca and L. Beirão Da Veiga, Virtual element methods for parabolic problems on polygonal meshes. *Numer. Methods Partial Differ. Eq.* **31** (2015) 2110–2134.

[50] M. Vohralik and B.I. Wohlmuth, Mixed finite element methods: implementation with one unknown per element, local flux expressions, positivity, polygonal meshes, and relations to other methods. *Math. Models Methods Appl. Sci.* **23** (2013) 803–838.

[51] E.L. Wachspress, Barycentric coordinates for polytopes. *Comput. Math. Appl.* **61** (2011) 3319–3321.

[52] J.A. Wright and R.W. Smith, An edge-based method for the incompressible navier-stokes equations on polygonal meshes. *J. Comput. Phys.* **169** (2001) 24–43.